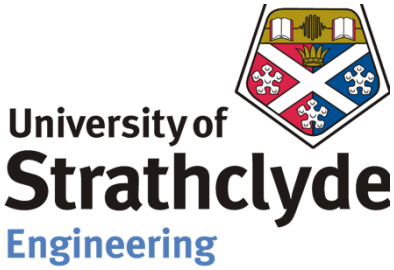

Department of Mechanical and Aerospace Engineering

Modelling and Analysis of Small Horizontal Axis Wind Turbine Blade Using Sustainable Material

Author: Laxmi Subedi

Supervisor: Dr. Emma Henderson

A thesis submitted in partial fulfilment for the requirement of degree in

Master of Science in Sustainable Engineering: Renewable energy systems & the Environment

2022

Copyright Declaration

Signed: Laxmi Subedi Date: 2022/08/12

Abstract

Wind turbines are one of the non-conventional source of energy. Since the design of the blades greatly affects the amount of energy that can be harvested, the rotor is an essential component in the development of wind power plants. In present work, small-scale HAWT of 5 kW was analysed. Four distinct types of aerofoils: NACA 63(4)-421, NACA 2421, LS (1)-0417, and LS (1)-0421, were each investigated for their aerodynamic performance and NACA 63(4)-421 was selected for the analysis due to its better performance comparing to other profiles. Sustainable materials were examined and flax/Polypropylene composite of 40 % fibre volume fraction was selected because of its high fatigue strength comparing to others like hemp, jute composites. The orthographic properties of the composite was defined. Various form of the load acting on the turbine blade along with consequential stress developed on the turbine blade were studied in line with IEC 61400-2 load condition. Among different load cases, parking load condition was considered for blade analysis and calculation of fatigue life. The geometry of wind turbine blade was created in SolidWorks and the finite element model of blade was analysed in ANSYS software. Structural and fatigue failure analysis was performed iteratively by varying the shell thickness to achieve a blade that satisfied the recommended safety factor. As the blade rotates the forces acting on it varies due to the change in direction of gravitational load with varying blade position. So, the blade was analysed at three different position of blade i.e. horizontal, topmost and bottommost to determine the fatigue life, accumulated damage and safety factor. Finally, result obtained from the ANSYS was compared with the value obtained from simple load model.

Keywords: Wind turbines, NACA 63(4)-421, NACA 2421, LS (1)-0417, LS (1)-0421, SolidWorks, ANSYS, IEC 61400-2, static analysis, fatigue analysis, safety factor

Acknowledgement

I would like to thank Dr. Emma Henderson, my academic advisor, for her important suggestions, ongoing support, and patience while I worked on my individual thesis. I am thankful towards her for allowing me freedom to choose topic of my interest and providing me base to do so. Her immense knowledge and insight encouraged me all the time through the dissertation.

Further, I would like to acknowledge Gemma Houston for her thoughtful comments and recommendations on this thesis.

At last, a special thanks to my parents for their constant source of inspiration and understanding throughout my research and report writing.

Table of Contents

Table of Figures

Nomenclature

Symbol	Description	Units
ρ	Air density	Kg/m^3
α	Angle of attack	Degree (°)
V_{AMWS}	Annual mean wind speed	m/s
V, V_{design}	Design wind speed	m/s
ω	Rotational speed	Rad/s
R	Blade radius	m
P_t	Turbine power	Watt
P	Wind Power	Watt
A	Rotor swept area	m^2
c	Chord length	m
ν	Kinematic viscosity	m^2/s
L	Lift force	N
D	Drag force	N
g	Acceleration due to gravity	m/s^2
m_{blade}	Mass of blade	kg
x	Distance between hub and centre of gravity	m
V_{hub}	Wind speed at hub height	m/s
V_{anemo}	Wind speed at anemometer height	m/s
Z_{hub}	Hub height	m
Z_{anemo}	Anemometer height	m
Z_0	Surface roughness length	m
S	Alternating stress amplitude	MPa
Vref	Reference wind velocity	m/s
Ve50	Extreme wind speed	m/s

Acronyms

Symbol	Description
VAWT	Vertical Axis Wind Turbine
HAWT	Horizontal Axis Wind Turbine
IEC	International Electrotechnical Commission
Re	Reynold number
C_L	Lift coefficient
C_D	Drag coefficient
C_P	Power coefficient
AoA	Angle of Attack
TSR	Tip speed ratio
IGES	Initial Graphics Exchange Specification
NACA	National Advisory Committee for Aeronautics
N_i	design number of cycle
n_i	Reference number of cycle
D	Damage
FEA	Finite Element Analysis
CAD	Computer Aided Drawing

1.0 Introduction

Background

Due to the ongoing fossil fuels depletion and the consequences of emissions on climate change, renewable energy is becoming increasingly important. Natural calamities induced by rising temperatures are growing in recent years, and as international environmental rules have been strengthened, eco-friendly technology that can cut CO_2 emissions are arising. Energy providers have invested in the development of wind turbines as they recognise the potential of wind energy. Only wind energy has grown more rapidly than anticipated among all renewable energy sources. In comparison to other renewable resources, wind energy has several benefits, such as relatively mature technology, cheaper, and wide range of resources. Furthermore, unlike solar energy, the utilisation is not influenced by environmental conditions like climate change and weather condition. The pace of growth in wind generating capacity over a 20-year period is seen in Figure 1. Globally, wind turbine of 837 GW capacity was installed by the end of 2021(IEA World Energy Outlook, 2021). By 2050, it is anticipated that onshore wind power generation capacity will reach around 5000 GW (Irena, 2019) while offshore wind power generating capacity will be about 1400 GW.

(Source: GWEC – Global Wind Energy Council)

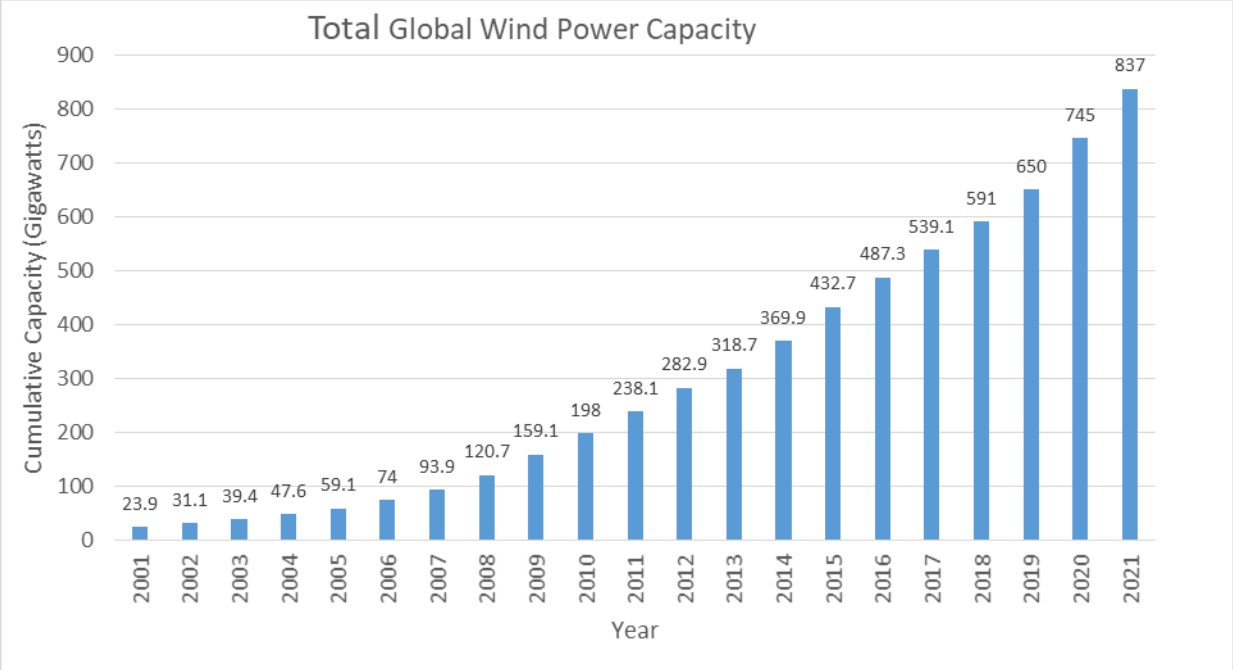

Figure 1: Total installed global wind power capacity from 2001 to 2021

Engineers invented the wind turbine for the energy extraction from wind. Wind turbines generate mechanical energy from moving air without using fossil fuels (Cao, 2011). Due to the

advancement in technology there is rapid growth in the energy generation from the wind. During design, several wind turbine components must be considered, including the tower, rotors, hub, and base designs. Today's taller turbines can harvest more wind at higher heights economically because of new developments in taller towers construction using stronger, lighter materials and better turbine design methods. The latest generation of wind turbine blades may reach 100 metres in length because of the use of composite materials, which has reduced the cost of energy production and increased turbine efficiency. It is essential to keep enhancing the wind turbine's design in order to maximise energy production and reduce costs.

The turbine wheels, tower, generator, driven chain, control system, and other essential components comprise a wind turbine. The great majority of current wind farm components are made up of materials like steel, iron, copper and aluminium which are recoverable and recyclable. However, about 10-16% of the total wind turbine mass is made up of glass fibre composites or carbon fibre which are hazardous, expensive to produce, and tough to get rid of when a product's usable life has expired (Mishnaevsky et al., 2017). The use of naturally sourced fibres is gaining increasing research interest in the designing and manufacturing of composites for the rotor blades (Verpoest, 2012). Natural fibres have several benefits over glass and carbon fibre composites, including their great availability and sustainability, their capacity for recycling, and their relative affordability (Bensadoun et al., 2016). Significant experimental research have been conducted in recent years to examine the properties of natural fibre. However, there has been minimal investigation into using natural composites for structural design. Incineration, disposal, and recycling of synthetic composite materials are increasing the need to use more easily recyclable materials in wind turbine blades from the start of the design process.

Due to unavoidable sky high electricity bill, wind energy is gaining popularity in small scale systems to improve the energy independence and to promote the local economy (UCL, 2022). Small wind turbines are intended for use in home, agricultural, small commercial, and certain industrial purposes. They are normally less than 50 kW in size, however they may reach capacities of 250 kW. Unlike large HAWTs, small HAWTs are built for power production without the influence of varying wind speed (Muhsen, Al-Kouz and Khan, 2019). Since small HAWTs perform poorly compared to large wind turbines, designing one needs a thorough understanding of the design parameters. The performance of the small HAWT is restricted by the workable state at less wind velocity and blade dimensions, resulting in a low Reynolds number and the possibility of viscoelastic separation on the blade (Singh and Ahmed, 2013).

The tiny size, fluctuating wind speed, and rapid rotating speed of small HAWT make them vulnerable to fatigue especially in urban environments (Song et al., 2018). As a result, it's critical to perform careful analysis of aerodynamic performance as well as static and fatigue analysis during blade design (Sarkar et al., 2019).

1.1 Aims & Objectives

Aims:

The primary goal of this thesis is to conduct an aerodynamic study of the rotor blades for a small horizontal axis wind turbine with a power output of 5 kW made of natural flax fibre and polypropylene composite. To assess the structural integrity of the blade, the blade was modelled in SolidWorks and static and fatigue analyses were done using the finite element method with ANSYS.

Objectives:

The main objectives of this report are as follows:

1. To carry out the aerodynamic performance analysis of different aerofoils.
2. To select the specific proper aerofoil with maximum lift-drag ratios.
3. To derive optimal aerodynamic parameters essential for blade design using BEM theory.
4. To calculate the material properties for composite blade.
5. To design the blade and carry out the structural and fatigue analysis.
6. To determine structural and fatigue damage safe optimal blade thickness.

1.2 Overview of the report

This work comprises of five chapters in total. In first chapter, an overview and current status of wind turbine, the main aims and objectives as well as the overview of the thesis was defined. In second chapter, literature review was done to investigate more about aerodynamic performance analysis, geometry creation, load definition, material selection and the failures occurring on the blade. Third chapter contains the methodology used for the present work. With the investigation of rotor design parameter, comparison was made between four selected aerofoils: NACA 63(4)-421, NACA 2421, LS (1)-0417 mod, and LS (1)-0421 mod to have the one with better aerodynamic performance. Following that suitable natural flax fibre and Polypropylene polymer matrix composite was selected, CAD geometry was created, and analysis was performed with material definition at different load condition. The result from the

analysis in FEM software was evaluated with different thickness of aerofoil shell to comply with safety limits. Chapter four and five and six, summarised the main findings and discuss potential ideas for future work in relation to the research and analysis.

2.0 Literature Review and Background Theory

A wind turbine is a rotating device that uses an electric generator, gear drive, and motor rotor to transform the kinetic energy of the wind into electrical energy (Cao, 2011). There are multitude of factors from aerodynamics to material selection to structural and fatigue optimization that influence the effective design of wind turbine. In this chapter, literature review was done to investigate more about those influencing factors.

2.1 Wind turbines Classification

The location of the shaft and the rotating axis of the blades determine the first categorization of wind turbines. It is divided into vertical axis wind turbines and horizontal axis wind turbines. Unlike VAWT, where the blade spins on an axis perpendicular to the ground, HAWT mounts the shaft in a horizontal position parallel to the ground as shown in figure 2.

Figure 2: Types of wind turbines according to position

Both types have a variety of designs that are available, and each kind has pros and cons. HAWT provides a number of benefits, such as high power output, high operational wind velocity, high reliability and low cost per unit power produced (Hyams M.A, 2012). A significant benefits of VAWT is their electricity production capacity regardless of wind direction. Because the generator, transmission, and other important turbine components are positioned on the ground, there is no need for a robust supporting tower, minimising the total cost of turbine. However, low tip speed ratio and challenging rotor speed management are responsible for the VAWT's mainstream development being abandoned. Another shortcoming is that when initiating, the blades of vertical-axis wind turbines must be rotated by an external energy source (Dominy et al., 2007). Only one end of the wind turbine's axis is supported at the ground, which

restricts maximum feasible hub height (Tong, 2011). Also, the wind power efficiency of VAWT is inferior comparing to HAWT which make it less commercially available.

2.2 Wind turbine design parameters

The distribution of chord and twist angle of each blade sections are highly influenced by the operating parameters as well as the blade aerofoil. The design wind speed, operational span of Reynolds numbers, the design power coefficient, rotor tip speed ratio and attack angle are a few of these crucial characteristics (Tenghiri et al., 2018).

2.2.1 Wind speed

Power that can be extracted from wind is directly proportional to cube of wind speed which makes wind speed as the critical characteristic in the generation of power. In reality, wind speed fluctuates throughout time and location, depending on a variety of factors such as geography and weather. As wind speed is an unpredictable characteristic, observed wind speed data is generally analysed statistically Tong, 2011). There is no standard connection to anticipate the annual mean wind velocity variation because it strongly relies on a few selected areas. Design wind speed is the wind speed over which the rotor of a wind turbine spins with maximum power coefficient. The annual mean wind speed, V_{AMWS}, should be 1.4 times the design wind speed, V_{design}, as shown in equation [1], in accordance with the IEC 61400-2 standard (IRENA, 2019).

$$V_{design} = 1.4\ V_{AMWS} \quad [1]$$

2.2.2 Number of Blades

The essential parameter for the design of turbine is blade number as it impacts the power output and the blade speed (Muhsen, Al-Kouz and Khan, 2019). The amount of energy that can be collected from the wind directly relates to the swept area of the blade; consequently, the number of blades has a direct influence on power output. As blade number increases drag force increases due to more resistance to wind flow causing the reduction in rotational speed of blades. Thus, power generation will be greater with the turbine having minimal blades. The HAWT usually has three blades. Wind turbine with one blade will have less drag and maximum efficiency but it is not practically possible as it causes imbalance (Kerrigan,2018). In two bladed turbine there will be an unstable torque occurring at the centre of the blade which made it more prone to the vibration leading to sudden damage (Adeseye Adeyeye, Ijumba and Colton, 2021). With the three and higher blade number the mechanical characteristics of turbine

will remain same in practice for every possible orientation of blade. On a certain size turbine, a maximum of four blades will result in higher power production. But, it results in excessive manufacturing cost than three bladed turbines (Wang and Chen, 2008). Because of these reasons, three-bladed turbine provides the perfect balance of high power production, excellent stability, light weight, and turbine longevity. Figure 3 shows how the blade number will impact on the wind turbine performance along with the performance of VAWT comparing to HAWT.

2.2.3 Tip speed ratio

It is the ratio of tangential wind velocity at the tip of the blade to the actual wind velocity. Efficiency is correlated with the tip speed ratio, with the optimal value varied with blade design. Three bladed wind turbine with high efficiency usually have tip speed ratio of 6 to 7 (Tabesh and Iravani, 2006). Higher tip speed ratios produce more noise and necessitate stronger blades owing to greater centrifugal forces. The structure will be at the risk of failure due to high stresses on blade. If the tip speed ratio is too low the blade will often slow down or stall (Singh and Ahmed, 2013). The attack angle that produces the best L/D ratio is optimal. Because the angle at which the wind hits the blade is determined by the velocity and wind direction, there is an optimal tip-speed ratio (Tenghiri et al., 2018) which is given by equation [2].

$$\text{TSR} = \frac{\text{Blade tip speed}}{Actual\ wind\ speed} = \frac{\omega R}{V_{hub}} \quad [2]$$

Where, ω is the rotational speed of the blade in radian/second, R is the rotor radius in meters and V_{hub} is the wind speed at hub height in meters per second.

2.2.4 Power coefficient

According to the Betz coefficient, the highest proportion of energy that may be collected from an undisturbed wind stream is 59.3 percent (Adaramola, 2021). Due to numerous losses caused by blade surface roughness, friction, and mechanical degradation, only around 35 to 45 percent of the energy can be drawn in practice (Rao, 2019). The Betz limit is an idealisation and a design objective that engineers aim to achieve while creating a turbine. It is the ratio of the power recovered by the turbine to the total energy available in the wind stream as shown in equation [3].

$$Cp = \frac{P_t}{P} = \frac{P_t}{\frac{1}{2}\rho A V^3} \quad [3]$$

Where, 'ρ' is the density of air, 'A' is swept area and 'V' is the design velocity.

The tip speed ratio and blade pitch often affect power coefficient. Considering pitch angle as zero, the plot between tip speed ratio and power coefficient for vertical wind turbine and horizontal wind turbine of different blade numbers (Hau,2013) can be seen in the figure 3.

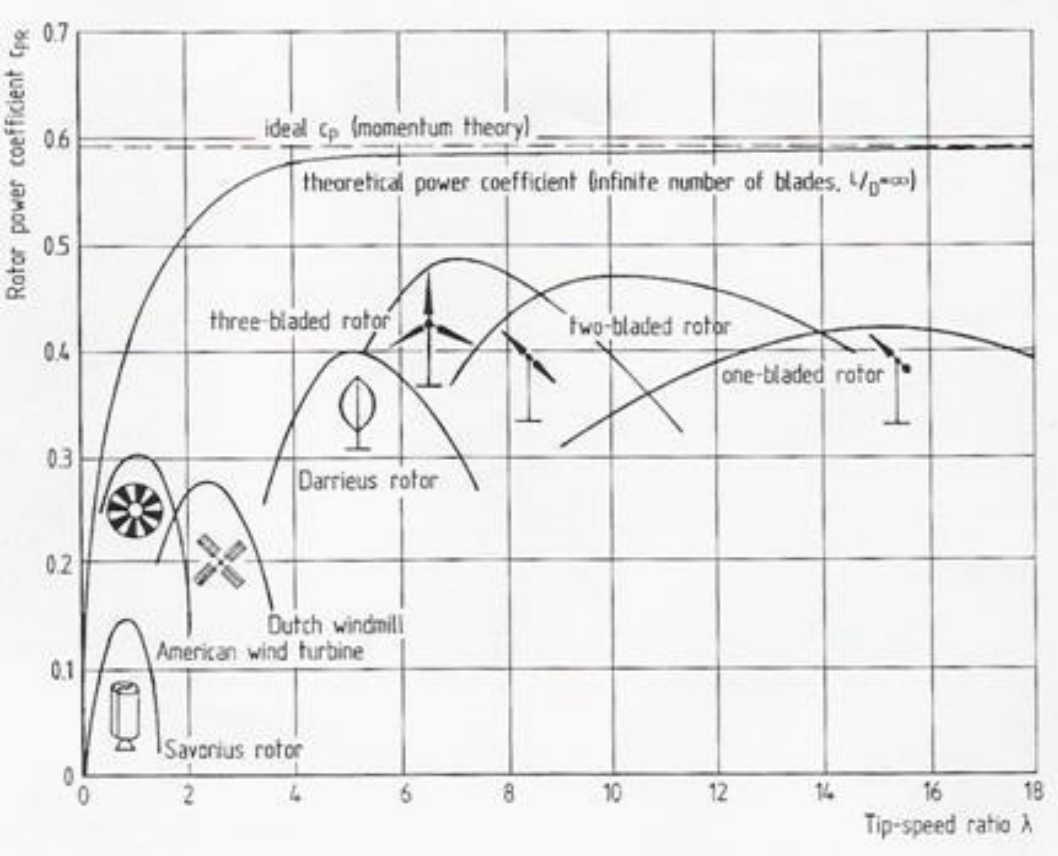

Figure 3: Rotor power versus tip speed ratio

2.2.5 Non-dimensional parameters

The use of non-dimensional parameters to characterise aerodynamics issues has been demonstrated through theory and investigation. The most essential parameter for fluid flow characterization is the Reynold number. Small-scale wind turbines behave aerodynamically quite dissimilar from large-scale wind turbines (Karthikeyan and Suthakar, 2016). An aerofoil's Reynolds number has a significant impact on how well a wind turbine performs aerodynamically and is calculated by equation [4] as:

$$\mathrm{Re} = \frac{\mathrm{Vc}}{v} \qquad [4]$$

Where, 'Re' is Reynold's Number, 'V' denotes freestream wind velocity, 'c' represents chord length and $'v'$ is kinematic viscosity of air; $1.511*10^5$ m^2/s. Small-scale wind turbines perform better with lower Reynolds numbers comparing to the large-scale wind turbines. Furthermore,

when the Reynolds number decreases, the peak lift coefficient decreases, while the drag coefficient marginally increases, indicating a rapid decrease in the L/D ratio, resulting in insufficient effectiveness for smaller horizontal axis wind turbines (Kishore, Coudron and Priya, 2013). The design of a small wind turbine with stall regulation should thus use an aerofoil shape with the greatest L/D ratio.

In most cases, rotors design make the use of two-dimensional coefficients that have been established through wind tunnel testing at a variety of angles of attack and Reynolds numbers (Hau,2006). The two dimensional lift and drag coefficient is calculated using equation [5] and [6] as:

$$C_L = \frac{L}{\frac{1}{2}\rho\, AV^2} \qquad [5]$$

$$C_D = \frac{D}{\frac{1}{2}\rho\, AV^2} \qquad [6]$$

Where, 'ρ' is the density of material, 'V' is undisturbed air velocity and 'A' is projected area of blade span. The power output generated by the turbine is determined by aerodynamic lift force acting perpendicular to the direction of flow, and it is critical to optimise this value using the suitable design. A resistive force called drag that opposed the blade motion needs to be minimised. Thus, one of the most important factors is the L/D ratio, which should be more than 30 for rotor blade design (Griffiths, 1977).

Although it is difficult to forecast the lift and drag coefficients numerically, tools such as JAVAFOIL and XFOIL are freely accessible to precisely simulate the aerofoil with the absence of post stall, huge attack angles, and the conditions of aerodynamic thickness (Adaramola, 2021).

2.2.6 Blade aerofoil

Variety of parameters are used for the characterization of aerofoil. The mean camber line is the locus of points located midway between the top and bottom surfaces of the aerofoil. The most forward and backward locations of the mean camber line are found on the leading and trailing edges, respectively. The aerofoil's leading and trailing edges are connected by a straight line known as the chord line. The distance between the leading and trailing edges of an aerofoil, as measured along its chord line, is known as its chord. The maximum thickness is defined as the largest distance between the top and bottom surfaces, determined normal to the chord line.

Angle of attack is the angular relationship between the chord line and the relative wind. (Manwell et al. 2010).

(Source: Olivier Cleynen, 2011)

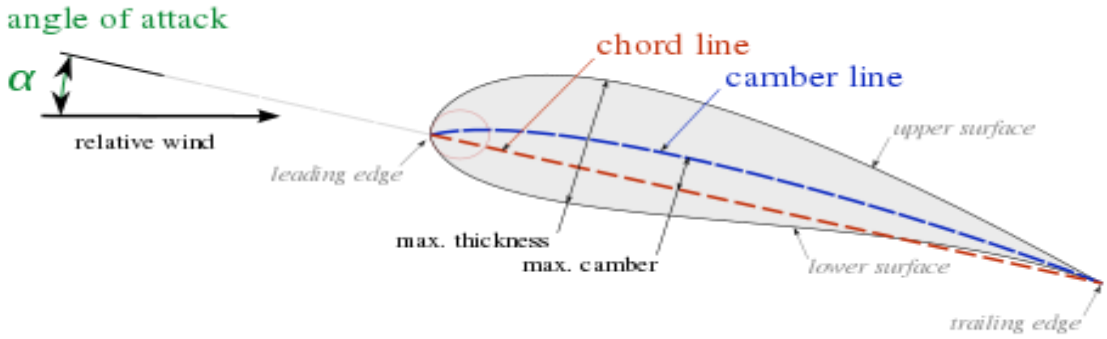

Figure 4: Aerofoil cross-section

The angle of attack with greatest L/D ratio is often chosen as the design angle of attack. However, the design angle of attack should be somewhat smaller than the ideal angle of attack with high L/D ratio. This technique prevents the aerofoil from entering fast into the stall zone with the increase in wind speed while allowing the blade to run at angles of attack that are close to the optimal value (Tenghiri et al., 2018).

2.2.7 Blade aerodynamics

Aerodynamic is essential for the wind turbines to function effectively. When wind blows through the aerofoil shape of the blade it produces two aerodynamic forces namely lift and drag. The profile of an aerofoil determines the chord wise distribution of lift which has an important role on blade aerodynamic performance (Maalawi and Badr, 2003). So, the proper selection of aerofoil is crucial for the design to be aerodynamically efficient. In the past, aerofoils are often evaluated experimentally using tables that correlate lift and drag at specific angles of attack and Reynolds numbers. Aerofoil designs for wind turbines have historically been adapted from those for aeroplanes with comparable Reynolds numbers and section thicknesses suited for circumstances near the blade tip (Adaramola, 2021). However, due to the variations in operating circumstances and mechanical stresses, extra considerations should be addressed while designing aerofoil profiles particular to wind turbines.

2.2.8 Blade structure

Typically, wind turbine blades and nacelles are made of composite materials (Mishnaevsky et al., 2017). The aerodynamic efficiency necessary to effectively collect energy from the wind

and the strength necessary to resist the stresses on the blade are what decide the shape and size of the wind turbine's blades (Bharambe and Bharambe, 2018). A wind turbine blade has two faces (on the suction and pressure sides), which are joined together by one or more integral (shear) webs connecting the bottom and top sections of the blade. Wind pressure causes the flap wise load, while gravitational forces and torque load cause the edgewise load.

On the pressure side of the main spar, one of the principal laminates is subject to cyclic tension-tension loads, whilst on the suction side, it is subject to cyclic compression-compression stresses. The laminates holding the bending moments associated with gravity loads are subjected to tension-compression loads at the leading and trailing edges. The sandwich-structured aero shells are made to withstand the buckling in particular. Different materials being used for various regions of the blade may be beneficial, according to the varied cyclic loading histories that have been seen at various points on the blades. In this work, due to time limitation, design complexity and higher simulation time requirement the spar web and the shear cap was not considered.

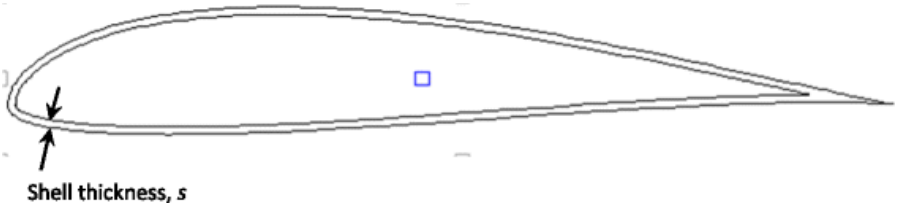

Figure 5: Schematic of wind turbine blade

2.2.9 Wind turbine blade material

Wind turbine blade plays a vital role in the wind turbine design. For maximum torque generation to run the generators it is essential to have an optimum cross-section of blade for higher efficiency. The efficiency of the turbine mainly depends on the type of material used, aerofoil shape and the angle of the blade. Therefore, the material for turbine blades should be chosen in such a way that it can withstand bending while being light enough to have a slow start-up speed. It should possess high stiffness, low density and longer fatigue life features (Budynas, Nisbett and Shigley, 2020).

A wide range of synthetic materials like carbon fibre reinforced polymers, glass epoxy composites and nanocomposites are available as blade material. Nowadays there is continuous research underway which leads to the development towards light weight and low life cycle cost materials. Composite materials are getting popularity due to their performance like low density with high resistivity to impact and low cost. Both mechanical and physical properties of

composites are better comparing to the other construction materials. Mostly glass fibre reinforced plastic (GRP) composites, carbon filament-reinforced-plastic (CFRP) are in used today with the continuous evolvement of turbines. But, there is scope for the improvement of the materials considering the recyclability factor. Certain plant stem fibre like fibre extracted from flax, jute, hemp, sisal have demonstrated significant potential to replace conventional synthetic fibres as reinforcement in engineering composites while still being environmentally safe and sustainable (Corbière-Nicollier et al., 2001). Although natural fibres like jute, hemp and from other plant stem are more susceptible to the variation in quality, high moisture take up and low thermal stability which makes them undesirable for large turbine blades they can still be advantageous to small wind turbine blade.

A prior study by Herrera-Franco et al. investigated at the mechanical characteristics of henequen, a natural fibre. The mechanical behaviour of high-density polyethylene reinforced using continuous henequen fibres was examined. (Herrera-Franco and Valadez-González, 2004).

The study by Dong examined natural fibre reinforced hybrid composites. The usage of hybrid/synthetic or hybrid/hybrid fibres to reinforce thermoplastic and thermoset composites was considered. The characteristics of natural fibres, as well as the characteristics and manufacturing of composites, were outlined (Dong, 2017).

Van den et al. investigated the effect of flax fibre physical structure on the mechanical characteristics of flax fibre reinforced Polypropylene composites. The elasticity and the strength of the material was determined through the experimental results and compared with the glass mat reinforced thermoplastic (Van den, 2000).

2.2.10 Wind turbine loads cases

Location affects how well a wind turbine performs. Since wind power is directly proportional to cube root of wind velocity, the turbine at the site with high velocity will have a tougher life and will suffer more from wear and tear. In order to work at their best and remain reliable over the course of their lifespan, the turbines must be designed for all weather situations. Manufacturers construct their wind turbines for a certain wind class to avoid having creation of too complex wind turbines that could all run reliably on all locations, regardless of how windy it was. The design classes has been specified by IEC for the small wind turbines with a rotor swept area less than 200 m^2 (Thong, 2000) which encompasses yearly average wind speed, turbulence model and severe wind speed as shown in table 1. The blade with same

length will have different designs to optimize the performance in high wind site and low wind site. So the choice of wind class is essential in the early stage of blade design.

Table 1: Basic parameters for small wind turbine classes (IEC,2005)

WTGS Class		I	II	III	IV	S
V_{ref}	(m/s)	50	42,5	37,5	30	
V_{ave}	(m/s)	10	8,5	7,5	6	Values to be
A	I_{15} (-)	0,18	0,18	0,18	0,18	specified
	a (-)	2	2	2	2	by the
B	I_{15} (-)	0,16	0,16	0,16	0,16	designer
	a (-)	3	3	3	3	

where:

- the values apply at hub height,
- A designates the category for higher turbulence characteristics,
- B designates the category for lower turbulence characteristics,
- I_{15} is the characteristic value of the turbulence intensity at 15 m/s,
- a is the turbulence slope parameter

A wind turbine must be examined for the various loads it will face throughout the course of its life span during the design phase. A main purpose of this is to make sure that the turbine can bear these loads with an adequate safety margin. This task is done by examining the wind turbine for a variety of load scenarios. Statistical models can be used for improving the process of estimation of design load. The load cases may be built by combining appropriate wind turbine design scenarios with diverse external variables. Basically, the design situation comprise up of numerous operating situations. To maintain the consistency of design-load conditions, standards have been developed by IEC. Eight alternative load situations are defined by the International safety standard for small - scale wind turbine's which establishes the load operating on the rotor blade. Usually extreme load condition among all the load condition (the extreme operating gust of 50 years) is used for designing and certification process (Rao, 2019). The table is provided in table 2.

Table 2: IEC design cases (IEC,2005)

Design situation	DLC	Wind condition[1]		Other conditions	Type of analysis	Partial safety factors
1) Power production	1.1	NTM	$V_{hub} = V_r$ or V_{out}		U	N
	1.2	NTM	$V_{in} < V_{hub} < V_{out}$		F	*
	1.3	ECD	$V_{hub} = V_r$		U	N
	1.4	NWP	$V_{hub} = V_r$ or V_{out}	External electrical fault	U	N
	1.5	EOG_1	$V_{hub} = V_r$ or V_{out}	Loss of electrical connection	U	N
	1.6	EOG_{50}	$V_{hub} = V_r$ or V_{out}		U	N
	1.7	EWS	$V_{hub} = V_r$ or V_{out}		U	N
	1.8	EDC_{50}	$V_{hub} = V_r$ or V_{out}		U	N
	1.9	ECG	$V_{hub} = V_r$		U	N
2) Power production plus occurrence of fault	2.1	NWP	$V_{hub} = V_r$ or V_{out}	Control system fault	U	N
	2.2	NWP	$V_{hub} = V_r$ or V_{out}	Protection system or preceding internal electrical fault	U	A
	2.3	NTM	$V_{in} < V_{hub} < V_{out}$	Control or protection system fault	F	*
3) Start up	3.1	NWP	$V_{in} < V_{hub} < V_{out}$		F	*
	3.2	EOG_1	$V_{hub} = V_{in}$, V_r or V_{out}		U	N
	3.3	EDC_1	$V_{hub} = V_{in}$, V_r or V_{out}		U	N
4) Normal shut down	4.1	NWP	$V_{in} < V_{hub} < V_{out}$		F	*
	4.2	EOG_1	$V_{hub} = V_r$ or V_{out}		U	N
5) Emergency shut down	5.1	NWP	$V_{hub} = V_r$ or V_{out}		U	N
6) Parked (standing still or idling)	6.1	EWM	$V_{hub} = V_{e50}$	Possible loss of electrical power network	U	N
	6.2	NTM	$V_{hub} < 0.7 V_{ref}$		F	*
7) Parked and fault conditions	7.1	EWM	$V_{hub} = V_{e1}$		U	A

1) If no cut-out wind speed V_{out} is defined, the value of V_{ref} should be used.

2.2.11 Design loads

As the turbine blade must be stiff enough to handle the load exerted on it, it is essential to determine the aerodynamic loads applied on the blade before performing the structural analysis. Basically, there are two methods for the prediction of aerodynamic loads: Blade element momentum (BEM) theory and computational fluid dynamics (CFD). BEM is the accurate and fast analytical method used for the initial design and load calculation while CFD is numerical

method which is preferred while performing the detail designing of blade. Now a days, different software's like LOADS, YawDyn, AERODYN are used for load calculation based on tip speed ratio, blade geometry and the condition of site (Habali and Saleh, 2000).

Wind turbine blades are susceptible to the loads due to its self-weight, wind force, centrifugal and gyroscopic forces. For the calculation of different types of load, the wind turbine blade is considered as the cantilever. To simplify the calculation, a worst case loading scenario can be identified and considered where rest of the load may be bearable. Size of the blade and control mechanism are the parameters on which the worst case condition is mainly depend. A 50-year storm condition is taken into account as the border case for small horizontal axis wind turbines without pitching of the blade (Gasch and Jochen Twele, 2012). Under this case, the types of loading on blade are (Burton, 2011):

1. Aerodynamic load
2. Gravitational force
3. Centrifugal force
4. Gyroscopic load
5. Operational load

The magnitude of these loads will depend upon the working condition considered during analysis. As turbine size increases the mass of the blade increases significantly at the cubic rate. So, gravitational load and gyroscopic load become critical for the large turbine blades. Gyroscopic load is mainly due to yawning of blade and generally less intensive comparing to gravitational load. And, operational load, a system dependent load which results due to pitching, breaking, yawning and the connection of generator can be comprehensive during emergency braking situation. Since, turbine in this case is small, so gyroscopic and operational was neglected as the blade capable of handling the aerodynamic, gravitational and centrifugal load can withstand these lessened load. Consequently, the following loads significantly affect the wind turbine's fatigue:

1. Aerodynamic load

Aerodynamic forces are used by all wind turbines for winds' energy extraction. It is the main force on the rotor blade that may be divided into two parts: lift and drag. An aerofoil's shape enables air to pass over it more quickly on top than it does at the bottom, which lowers the surrounding atmosphere's pressure. Because of the difference in air pressure the resulting lift force is generated. Additionally, drag force is produced as a result of the difference between

the blade and the air velocity. In order to reproduce the aerodynamic lift and drag forces, the BEM theory makes use of the lift and drag coefficients (Nguyen and Metzger, 2015). For the parked wind turbines the aerodynamic forces is calculated directly by using relative wind velocity which is given by equation 3 and 4.

$$L = \frac{1}{2} C_L \rho A V^2 \quad [7]$$

$$D = \frac{1}{2} C_D \rho A V^2 \quad [8]$$

2. Gravitational load

It is a mass dependent load which increases cubically with increase in turbine diameter (Brøndsted, Lilholt and Lystrup, 2005). It is the product of mass and acceleration due to gravity. The magnitude of this load will remains constant and acts towards the centre of the earth. Even the wind velocity acting on blade is considered constant the applied load on the blade swings between the maximum and minimum value as the result of variation of direction of gravitational load with respect to the local position of the blade. So, the gravitational force causes an alternating cyclic load case.

Gravitational load for each blade can be calculated as:

$$F_g = m_{blade} g \quad [9]$$

3. Centrifugal load

The centrifugal force on the blade transports the centrifugal force acting on the blade will try to persuade the air away from its circular path. Small wind turbine blades will experience larger centrifugal force but lower load variation due to gravity. Centrifugal load acting on individual blade can be determined as:

$$F_c = m_{blade} \omega^2 x \quad [10]$$

Where,

m_{blade} = mass of each blade

x= distance between the hub and centre of gravity of blade

ω = Angular velocity of rotor

g= Acceleration due to gravity

For the finite element analysis of the blade, gravitational force and centrifugal force are applied on the centre of gravity of blade while aerodynamic loads are implemented on the faces of blade.

2.3 Rotor blade failure mode

The development of wind turbines today is geared toward heavier and bigger constructions, which raises the failure frequency. Blades frequently experience alternating stress and diverse surroundings, and as a result, they frequently fail. The most common failures include wear, freezing, fatigue, fracture, and sensor failure (Tavner, Xiang and Spinato, 2007). The rotor blades elevated location makes maintenance, repair, and replacement expensive and complicated. Therefore, investigating the connections between various failure modes, reliability, and internal and external stresses is crucial. In this work, fatigue failure of the wind turbine blades was investigated into more detail.

Fatigue is a failure mechanism produced by cyclic load cycles with amplitudes less than the ultimate strength of the material. It is officially classified into three stages: crack initiation, crack propagation, unstable rupture and final fracture. The applied force can be either of constant amplitude or variable type. A repetitive force applied to a certain object under observation will eventually cause microscopic cracks in the material to spread gradually until the final failure of the material occurs. Fatigue damage is generally cumulative and so irreversible (Evans et al., 2020). Mainly the fatigue life of the material depends on the material properties, loading condition and the manufacturing process. According to the time required for the failure, fatigue is divided into two groups as high cycle fatigue and low cycle fatigue. The number of cycles necessary for failure in high cycle fatigue is greater than in low cycle fatigue. High cycle fatigue takes around 10^4–10^5 cycles (Germanischer, 2010) or more to reach. The reason for this is because if the applied stress is low and close to zero, the component will remain mostly in the elastic zone and will require more cycles. However, if the load exceeds the yield strength, the component will be pushed plastically, requiring fewer failure cycles, and a low cycle fatigue failure will occur.

A thorough explanation of the fatigue load spectrum and fatigue behaviour is necessary for the damage analysis of rotor blades. Numerous different forms of fatigue loading exist, including complete reversal cyclic loads (tension-compression loads), repeating cyclic loads (zero to tension loads), pure cyclic loads (tension-tension or compression-to-compression loads), and irregular or random load cycles (Kumar, Krishnan and Vijayanandh, 2018). To study the

fatigue phenomena, three approaches were developed. The Stress-Life approach is the first one. This approach doesn't take into account the impacts of fracture initiation or propagation. For analysis, the material's Stress versus Cycle (S-N) curve is employed. The component fails when the damage value is, for example, equal to one for Palmgren- Miner's damage rule. Strain-Life is another technique. Using strain versus cycle graphs, fracture start is examined as a failure criteria in this technique. The Fracture Propagation approach, which estimates the whether the crack is present or not and then examines its growth using Linear Elastic Fracture Mechanics, is the last method (Aykan, 2005).

The wind turbine rotor blades are often considered as the crucial component of a wind turbine system (Huque et al., 2012). The fatigue life of the blades must be carefully taken into account by designers when creating structures, and full-size structures must be tested. The IEC 61400-1 international specification and the Germanischer-Lloyd (GL) (Kong, Bang and Sugiyama, 2005) regulations specify design requirements such as limit for minimum blade tip clearance, limit in the stress and strain, and fatigue life time over its lifespan (Wang and Chen, 2008).

3.0 Methodology

From the literature review it was found that commercially the popularity of HAWT in an industry is higher due to several benefits. Thus, a HAWT was chosen for this study. The overall methodology followed from design to analysis is present in this chapter.

3.1 Aerofoil selection

Selection of proper aerofoil is the important of designing small wind turbines. With the increase in rotor size, Reynold number of an aerofoil profile will increase to reach a higher value. The Reynolds number is a dimensionless number used for flow characterization and is primarily used in the selection of the aerofoil (Clausen and Wood, 1999). Usually small wind turbines operate at Reynold number below $5*10^5$ because of its small radius. This value is found to be smaller at the tip of the blade (Mathew, 2011). In those range the laminal flow sets apart on top surface of the aerofoil which again attach to the surface as the turbulent resulting in laminar separation bubble. The bubble increases drag force, which has a substantial impact on aerodynamic performance. The complicated nature of the stream around the blades in low Reynolds numbers necessitates the careful selection of aerofoil profiles during the design of small wind turbine.

In present work, according to the recommendation from the literature review four different aerofoils were used for examination: NACA 63(4)-421, NACA 2421, LS (1)-0417, LS (1)-

0421. Being different shapes, they have different aerodynamics. Figure 6 shows the general aerodynamic profiles of those aerofoils.

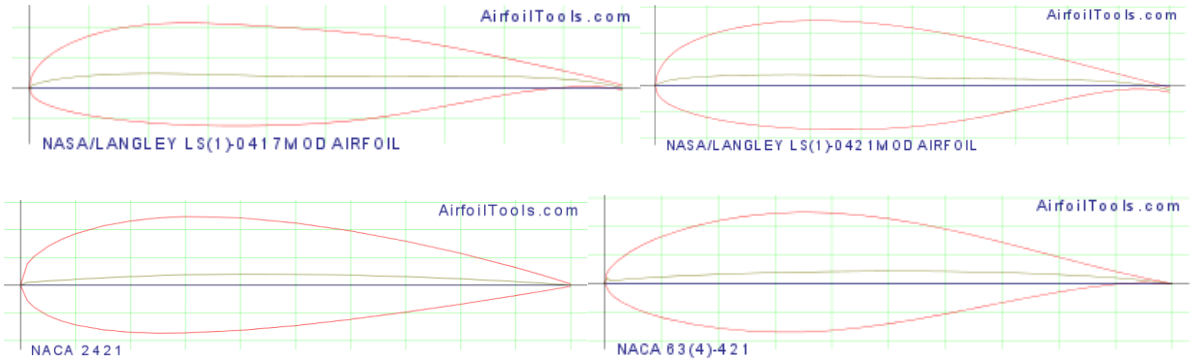

Figure 6: Aerodynamic profile of NACA and NASA/LS profiles

High lift force and low drag force are required for efficient wind turbine operation. Low attack angles result in significant lift forces and little drag forces. However, as the angle of attack exceeds a particular number, the lift force drops and the drag force rises. As a result, angle of attack is critical when building a blade (Benham et al., 2013). In this work, data required to determine the aerodynamic characteristic was imported to excel from XFOIL software to plot the graphs. The Reynold number effect on the aerodynamic performance of aerofoils was investigated among the four aerodynamic profiles. Here, the graph between the lift/drag ratios against the angle of attack from 0 to 20 degree for four different Reynold numbers; $5*10^4$, $1*10^5$, $2*10^5$ and $5*10^5$ can be seen in the figure 7, 8, 9 and 10.

It can be observed from the graph that the L/D ratio increases with the increasing value of Reynold number. L/D ratio is higher for the NACA63 (4)-421 aerofoil among the four with the value of 95 at 8.5° angle of attack. Peak L/D ratio value of LS (1)-0417 MOD and LS (1)-0421 MOD are found to be similar for the Reynold number of $1*10^5$, $2*10^5$ and $5*10^5$ but the peak value for LS (1)-0421 MOD is at smaller angle of attack. NACA 2421 shows the worst performance among four with the least values of L/D ratio although it follows the similar pattern to the LS (1)-0421 MOD for each Reynold number.

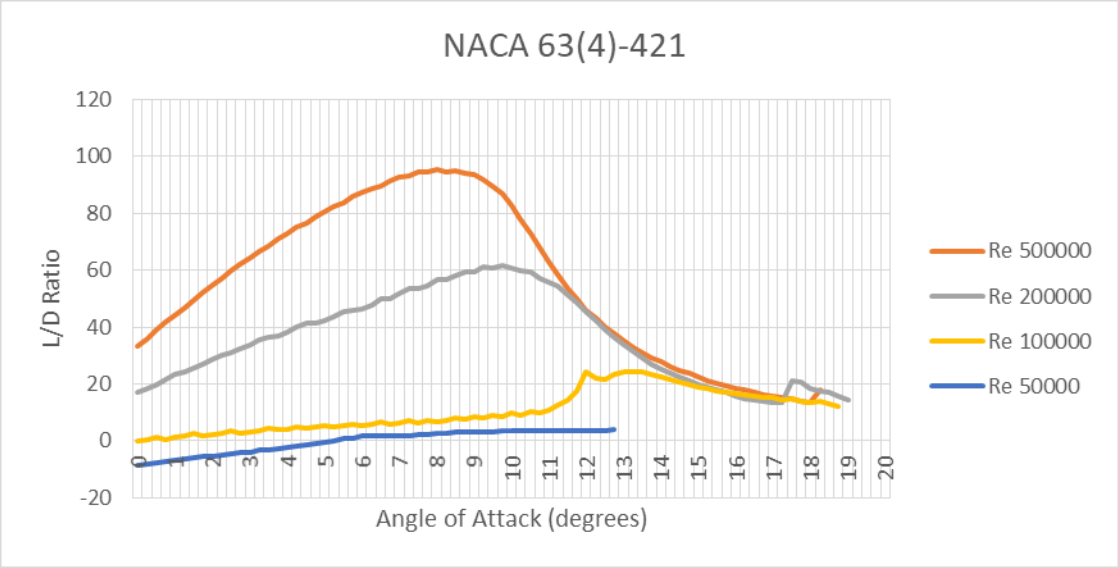

Figure 7: L/D ratio versus AoA for NACA 63(4)-421

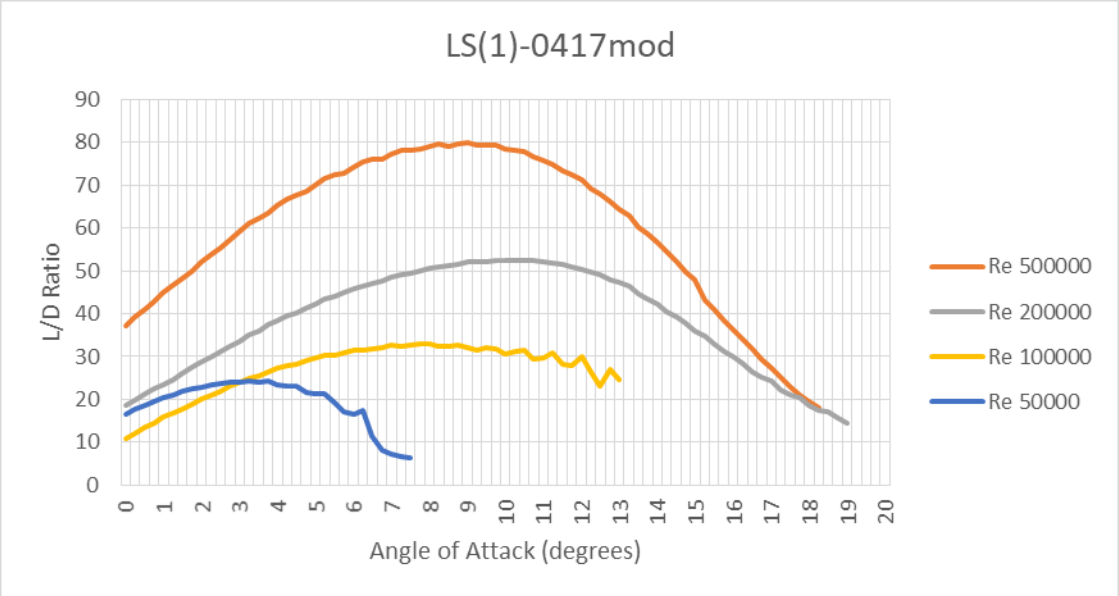

Figure 8: L/D ratio versus AoA for LS (1)-0417 mod

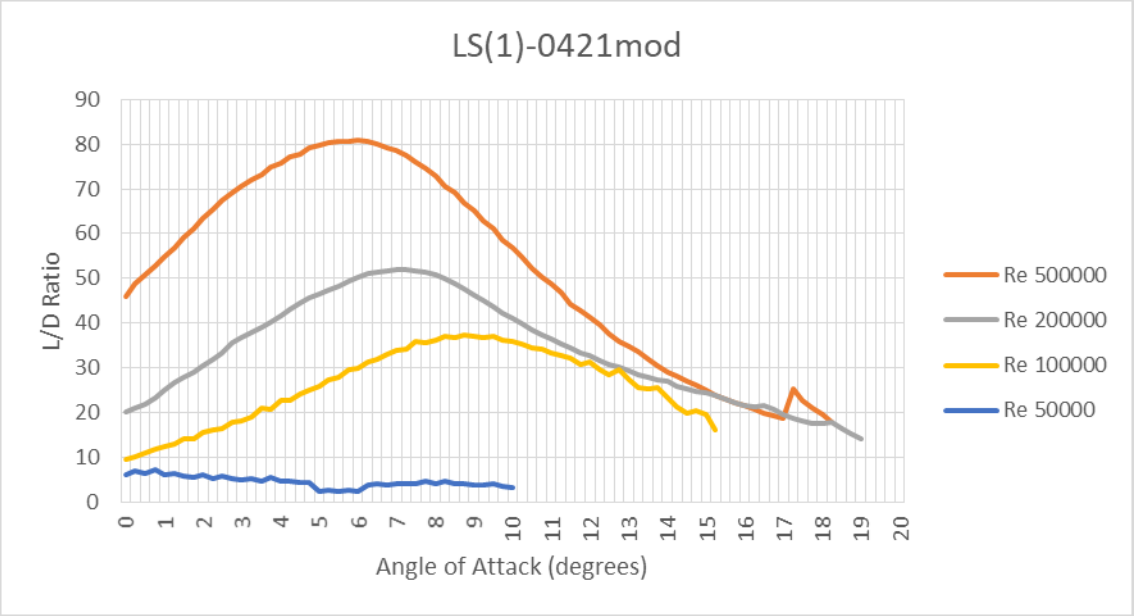

Figure 9: L/D ratio versus AoA for LS (1)-0421 mod

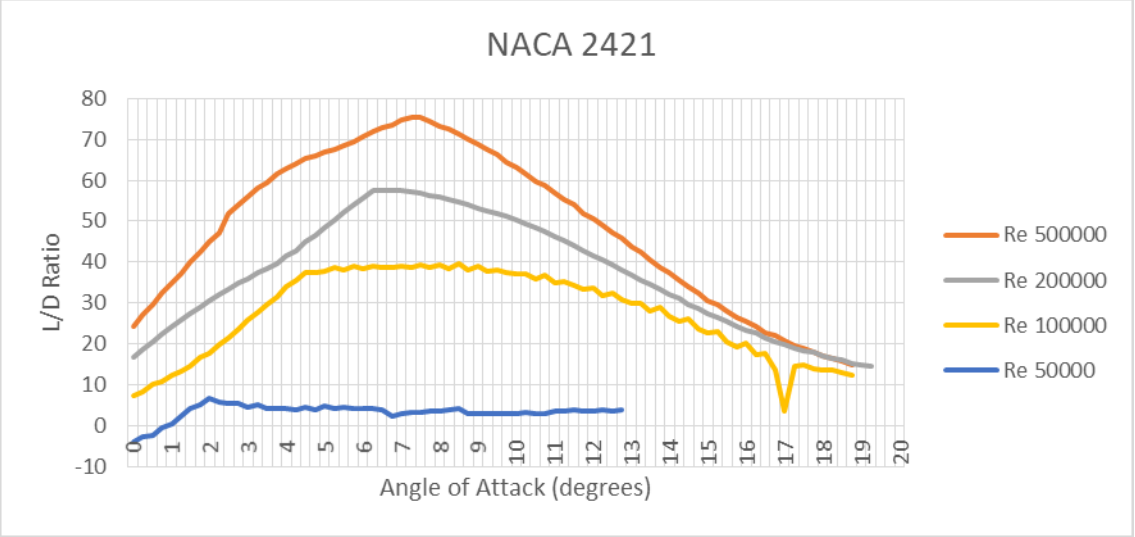

Figure 10: L/D ratio versus AoA for NACA 2421 mod

Due to high lift to drag ratio and smooth profile at different value of Reynold number over the range of angle of attack, NACA63 (4)-421 was selected which has maximum thickness 21% at 34.8% chord and maximum camber 2.2% at 50% chord for the further analysis. The graph was plotted between the lift coefficients and angle of attack with the range from -20° to 20° as shown in figure 11. And the graph between drag coefficients versus angle of attack was plotted as represented by figure 12.

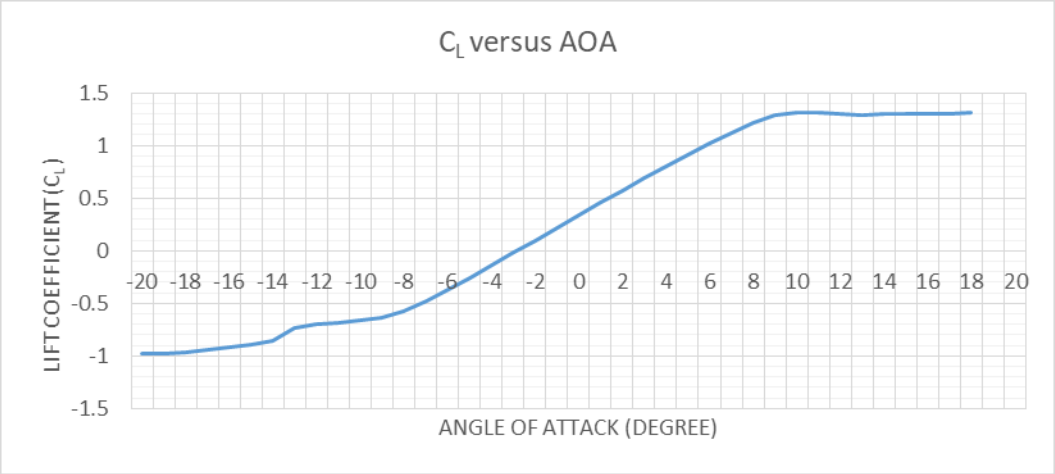

Figure 11: Lift coefficient versus Angle of Attack for NACA 63(4)-421

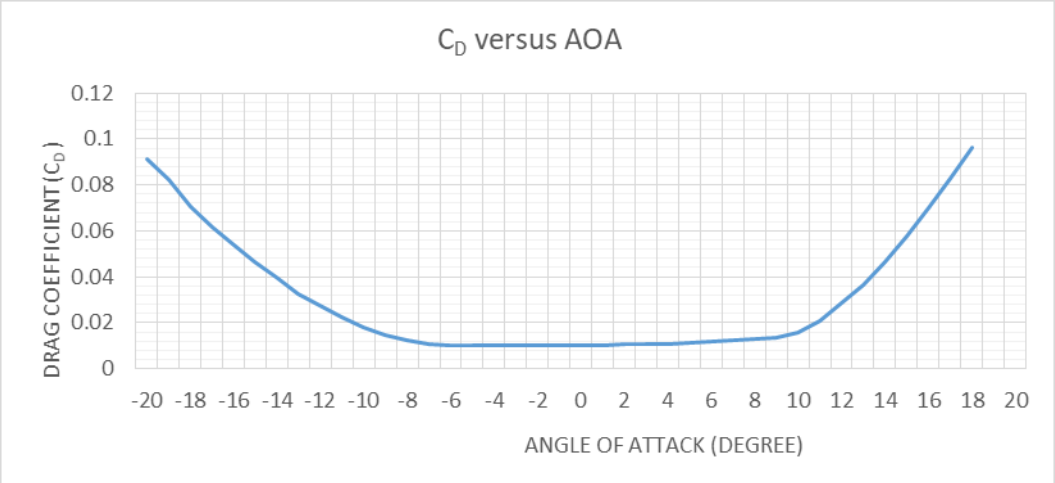

Figure 12: Drag coefficient versus AoA for NACA 63(4)-421

The lift and drag coefficient was taken from the graph as 1.254 and 0.013 which can be used for the calculation of the load in the later stage.

3.2 Blade design

Minimizing the overall cost is always desirable which leads to ease of manufacturing as one of the deciding criteria in blade design. Usually in large wind turbine blade multiple aerofoil profiles are used along the span of the blade with thicker blade at the root and thinner blade towards the rotor tip. However, due to complexity of design a single aerofoil was selected in this study which is usually done for small wind turbines. Along with that, angle of twist of rotor blade has marginal effect on the power output in small wind turbine and was neglected.

Wind speed is intermittent in nature and can be different at a particular height and area due to uncertainties like surface roughness, location and height above the ground. Accurate

predictions of wind speed at hub height will result in accurate calculations of energy output. In general, there are no observations of wind velocity at hub height. Therefore, approaches for correctly predicting wind speeds from other available measures must be investigated. In order to find the wind speed, recorded at a reference height, to the hub height, aerodynamic surface roughness, or z_0, is a crucial factor [Eduard Muljadi and H Edward Mckenna 2001]. The earth's surface roughness has an impact on how much slower the wind moves. Forests and huge towns plainly slow the wind significantly, but the water surface are much smoother and have less impact on the movement of wind, the value of which is presented in the table 3.

Table 3: Typical Surface roughness lengths (Saheb, Koussa and Hadji, 2014)

Terrain Description	Surface lengths (m)
Very smooth, ice or mud	0.00001
Calm open sea	0.0002
Blown surface	0.0005
Snow surface	0.003
Lawn grass	0.008
Rough pasture	0.01
Fallow field	0.03
Crops	0.05
Few Trees	0.10
Many trees, few buildings	0.25
Forest and woodlands	0.5
Suburbs	1.5
City center, tall Buildings	3.0

The average wind speed data available from meteorological observations was measured at the ground level (height of 10m). The houses in Scotland average a height between 4.7 to 5.8 m and the hub height needs to be at least 10m above from the roof of the house. So, the total hub height was taken as 16m in this case. The annual wind speed at ground level for the year 2021 was averaged in excel from the meteorological data available and found as 4.25 m/s. From that, mean hub height wind speed was determined by equation [11].

The logarithmic profile is based on the assumption that wind speed is related to the logarithm of height above ground (Saheb, Koussa and Hadji, 2014). The relationship between the wind speed at hub height and the wind speed at anemometer height is provided by the equation below.

$$\frac{V_{hub}}{V_{anem}} = \frac{\ln\left(\frac{z_{hub}}{z_0}\right)}{\ln\left(\frac{z_{anem}}{z_0}\right)} \qquad [11]$$

$$V_{hub} = 4.25 * \frac{\ln\left(\frac{16}{2.9}\right)}{\ln\left(\frac{10}{2.9}\right)} = 1.38 * 4.25 = 5.87\ m/s$$

Where,

V_{hub} = wind speed at hub height [m/s]

V_{anem} = wind speed at anemometer height [m/s]

z_{hub} = hub height of the wind turbine [m]

z_{anem} = anemometer height [m]

z_0 = surface roughness length [m]

ln (..)= natural logarithm

After calculating the annual mean wind velocity at the hub, the design velocity is calculated as:

$$V_{design} = 1.4V_{hub} = 8.22\ m/s$$

In order to determine the length of blade required it is essential to calculate the power available in the wind. For this case study, small horizontal axis wind turbine was considered with the power output of 5 kW. From the calculated design velocity and the power output the length of the blade required was determined as:

$$P = \frac{1}{2} C_p \rho A {V_{design}}^3 \quad [12]$$

Where,

C_p = Power coefficient (0.45, according to Betz law)

ρ = Density of air; 1.225 kg/m^3

A= Rotor swept area

V_{design}= design wind velocity

P= design power output

$$A = \frac{P}{\frac{1}{2} C_p \rho {V_{design}}^3} = \frac{5000}{\frac{1}{2}*1.225*0.45*8.22\text{^}3} = 32.65\ m^2$$

And,

A=πr^2 gives the radius of blade as 3.2 m.

After calculation of the blade length the next step was to find the optimum aerodynamic chord length. The chord length of a HAWT rotor blade was determined using the BEM technique in

correspondence with the Betz limit, regional local wind speed, and lift force (Hau, 2013). The best chord length can be determined using a variety of theories, the simplest of which is based on the Betz optimisation. When utilising aerofoil sections with low drag and tip losses, Betz's momentum theory yields a reliable estimate for blades with tip speed ratios of six to nine (Hau, 2013). For the cases of low tip speeds and the area near to the hub this method usually considered as unreliable. Losses due to drag and wake needs to be considered in that case (Gasch and Jochen Twele, 2012). The basic form of a modern rotor blades was shown via the Betz technique.

The blade usually has different aerofoil profile and width along its radius. The chord length over the blade was calculated by dividing blade into the sections of length 0.4m. The value of the lift coefficient was taken as 1.254 from the graph for the selected angle of attack. With the tip speed ratio of 7 the optimum chord length at different section of the blade is calculated using equation [13].

$$c = \frac{5.6 * R^2}{N * C_L * r * TSR^2} \qquad [13]$$

Where,

R= Radius of rotor blade

r= radius at the span wise location

C_L= Lift coefficient

TSR= Tip speed ratio

Reynold number for the calculated chord length was determined using equation [4] and tabulated as:

Table 4: Chord length and Reynold number at different location of blade span

Span-wise location	Chord length	Reynold number
0.4	1.54	667,806
0.8	0.77	333,687
1.2	0.51	222,458
1.6	0.39	167,060
2	0.31	133,734
2.4	0.26	111,229
2.8	0.22	95,215
3.2	0.19	83,530

Minimizing material consumption and manufacturing costs while boosting yearly energy output costs is critical for the continual adaption of tiny wind turbines (Jenkins et al., 2016). For this reason shear web and spar cap was not added for the analysis in this work.

3.3 Material selection

Composite material is the homogeneous structure that consists of fibre and matrix element as demonstrated as a block in figure (Christensen, 2005). The amount of fibre in a composite laminate has a considerable impact on its mechanical qualities. In general, increasing the quantity of fibre loading to an ideal value enhances the strength and Elastic modulus of the composite laminates. However, it falls as the fibre volume exceeds the optimum. The volume fraction of fibre was considered as 40 % in this case study as it is the maximum achievable value for the common hand lay-up process as the mechanical properties will start to degrade at higher fibre content. Common hand layup technique was used because it is simple and cheaper method (Mohd Bakhori et al., 2018).

The fibres of composite materials can be organised in a variety of ways, affecting the strength and stiffness of the material. To accommodate the bending of the blade, a wind turbine blade will have more fibres in the longitudinal direction and less in transverse direction. The variation in fibre orientation has made the research more complicated because even though fibres orientation in longitudinal transverse direction has less impact on the stress, it results in low strength due to less fibre.

Since the properties of the composite will be different depending upon the fraction of the fibres and matrix in the composite. One of the simple method for the prediction of elastic properties of composite is Rule of mixture which measures properties based on the contribution of each part of the composite (Marcal and Yamagata, 2016). Here, the volume fraction of aligned fibre with in the matrix is changed into the block of same volumetric fraction. The block is made up of two volumes, one representing the fibre (f) and the other the matrix (m), each having its own characteristic and volume proportion. The total volume fraction of composite is equal to the sum of fibre and matrix volume fraction. The theoretical values of the micromechanical properties of composite material is calculated based on the Rule of Mixture as described by Alger.

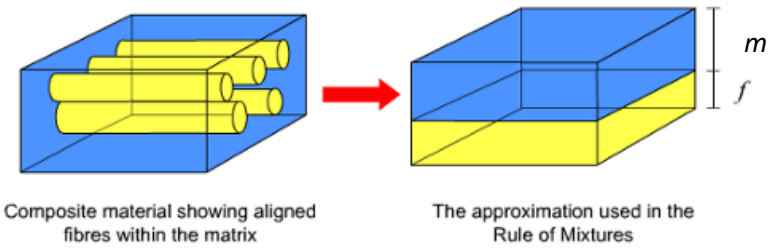

Figure 13: Alignment of fibre in matrix

Micro-scale analysis was used to investigate the parameters of unidirectional flax fibre matrix composites, in which the fibre was considered as transversely isotropic and the polypropylene as a two dimensional material having linear elastic properties. The properties of flax fibre utilized as input was summarised in table 5 (Le Duigou and Baley, 2014), (Andersons, Spārniņš and Joffe, 2009).

Table 5: Flax fibre material properties

Material Properties	**Flax fibre**
Longitudinal Modulus, E_{f11} (GPa)	54.1
Transverse Modulus, E_{f22} =E_{f33} (GPa)	7
Longitudinal Shear Modulus, G_{f12} = G_{f13} (GPa)	3
Transverse Shear Modulus, G_{f23} (GPa)	2
Major Poisson's Ratio, v_{f12}= v_{f13}	0.3
Minor Poisson's Ratio, v_{f23}	0.75
Tensile Strength in fibre direction, X_{fT} (MPa)	1000
Compressive Strength in fibre direction, X_{fC} (MPa)	830

The elastic modulus (E_m), shear modulus (G_m), tensile strength (X_{mT}), compressive strength (X_{mC}) and Poisson's Ratio (v_m) of the polypropylene as the matrix resin was considered as 1.6 GPa, 400 MPa, 36.1 MPa, 40 MPa and 0.4 (Notta-Cuvier et al., 2015), (Kellersztein and Dotan, 2015).

With the volume fraction of fibre (V_f) and of matrix (V_m), the density of the composites can be calculated as:

$$\rho_c = \rho_f V_f + \rho_m V_m \quad [14]$$

$= 0.4 * 1.5 + 0.6 * 0.9$

$=1.14\ g/cm^3 = 1140\ Kg/m^3$

The Chami's law has been used to evaluate the longitudinal modulus of elasticity and the strength and strain of the composites in the direction parallel to the fibre as shown by equations [15], [16], [17], [18], [19] and [20].

$$E_{ply11} = E_f V_f + E_m V_m \quad [15]$$

$$E_{ply22} = E_{ply33} = \frac{E_m}{1 - \sqrt{V_f(1 - \frac{E_m}{E_{f22}})}} \quad [16]$$

$$G_{ply12} = G_{ply13} = \frac{G_m}{1 - \sqrt{V_f\left(1 - \frac{G_m}{G_{f12}}\right)}} \quad [17]$$

$$G_{ply23} = \frac{G_m}{1 - \sqrt{V_f\left(1 - \frac{G_m}{G_{f23}}\right)}} \quad [18]$$

$$v_{ply12} = v_{ply13} = V_f v_f + V_m v_m \quad [19]$$

$$v_{ply23} = \frac{E_{ply23}}{2G_{ply23}} - 1 \quad [20]$$

For the calculation of yield strength, Hook's law for the composite was used and calculated as:

$$\sigma_{yc} = [1 + \frac{E_f V_f}{E_m V_m}] V_m \sigma_{ym} \quad [21]$$

$$(\varepsilon_f)_{ult} = \frac{(\sigma_f)_{ult}}{E_f} \quad [22]$$

$$(\sigma_c)_{ult} = (\sigma_f)_{ult} V_f + (\varepsilon_f)_{ult} E_m V_m \quad [23]$$

Where,

E_{ply11}= Composite longitudinal elastic modulus

E_{ply22}= E_{ply33}= Composite transverse elastic modulus

G_{ply12} = G_{ply13}= Longitudinal shear modulus

G_{ply23} = Transverse shear modulus

v_{ply12} = v_{Ply13} = Composite major Poisson's ratio

v_{ply23} = Composite minor Poisson's ratio

σ_{yc} = Yield strength of composite

σ_{ym} = yield strength of matrix

$(\varepsilon_f)_{ult}$ =ultimate strain of fibre

$(\sigma_f)_{ult}$ = ultimate strength of fibre

$(\sigma_c)_{ult}$ = ultimate strength of composite

Table 6: Material properties of uni-directional Flax/PP

Uni-directional Flax/PP Composite Properties		
Orthotropic Elasticity		
Elastic Modulus (GPa)	Shear Modulus (GPa)	Poisson's Ratio
E_{Ply11}= 22.98	G_{Ply12}= 1.04	v_{Ply12}= 0.38
E_{Ply22}= 3.03	G_{Ply23}= 1.06	v_{Ply23}= 0.7
E_{Ply33}= 3.03	G_{Ply13}= 1.04	v_{Ply13}= 0.38
Stress Limits		
Tensile Strength (MPa)	Compressive Strength (MPa)	Shear Strength (MPa)
σ_{T1} = 334.85	σ_{C1} = -246.34	τ_{12} =18.48
σ_{T2} = 31.6	σ_{C2} = -72.1	τ_{23} =18.33
σ_{T3} = 31.6	σ_{C3} = -72.1	τ_{13} =18.48
Strain Limits		
Tensile Strain	Compressive Strain	Shear Strain
ε_{T1}= 0.0146	ε_{C1}= -0.0107	ε_{12}= 0.0178
ε_{T2}= 0.0104	ε_{C2}= -0.0238	ε_{23}= 0.0173
ε_{T1}= 0.0104	ε_{C1}= -0.0238	ε_{13}= 0.0178

3.4 Failure cases

The fatigue requirement frequently affects main structural components design of a turbine since wind turbines need to have a 20 to 30 years of operational life to be cost effective (Kong, Kim and Park, 2014). Cycles to failure are commonly used to describe the repeated major stresses number that a structure can withstand it before emerging fractures. For the composite material, with the use of S-N characterization curve, the relationship between the stress amplitude and the number of cycles required for the component to fail can be shown graphically. The slope of the S-N curve often determines a material's fatigue characteristic. A flat S-N curve offers superior fatigue characteristics than elevated curve. Each S-N diagram is produced for a specific R-value since cycle amplitude significantly influences fatigue. Mao and Mahadevan discussed the composite material S-N behaviour at a constant stress ratio R is compatible with exponential relation that is linear in terms of maximum stress versus failure log cycles.

The Goodman diagram is the recommended classification for the study of S-N data. The constant failure cycles diagram are often, but not always, assumed to be straight lines between R-value lines (Sutherland, 2000). Since the Goodman diagram is not linear for blade material, the influence of mean stress is sometimes totally ignored when evaluating the damage to turbine blades.

The required optimal fatigue strength was first calculated, and the service life was then assessed using modified Spera's formulae (Kong, Kim and Park, 2014). Practical fatigue load spectrums can be derived from an analogous wind turbine system with Mandell's S-N diagram, and the Goodman diagram of composite materials. Equation [24] was used to assess the alternating stress for various cycle counts.

$$S = aN^{b} = 210.5N^{-0.005} \quad [24]$$

Where,

S=Alternating Stress

N=Number of cycles

a, b= Constant depends upon material

From the literature review, the value of 'a' and 'b' were taken as 210.5 and -0.005 which was found from the experimental results for flax/pp composite with the fibre fraction of 40% (Bensadoun et al., 2016).

Table 7: stress amplitude at different number of cycles for Flax/PP

Number of cycles (N)	Alternating Stress (MPa)
10	210.34
10^2	187.46
10^3	167.08
10^4	148.91
10^5	132.71
10^6	118.28
10^7	105.42
10^8	93.95
10^9	83.74
10^{10}	74.63

For the fatigue damage evaluation the IEC 61400-2 recommends the use of the Miner's law to determine accumulated damage. The total of the ratio between reference number of cycles, n_i, and the anticipated number of cycles, N_i, for all load range classes, is used to estimate the overall damage, or D, under the concept of linear damage accumulation. A component is meant to break when the damage is unity. The damage of a component is computed using the following equation (Sun et al., 2013).

$$D = \sum_{i=1}^{n} \frac{N_i}{n_i} \quad [25]$$

Here fatigue analysis was performed only at the extreme wind design condition without taking into account the effect of inlet wind variations. The average wind velocity for Scotland is 5.87 m/s which is near to V_{ave} of 6m/s so the design was analysed under IV class. Using the power law equation, the extreme wind speeds, V_{e50}, with 50 years recurrence time are to be undertaken for the stable strong winds scenario given by equations (IEC, 2005).

$V_{e50} = 1.4\ V_{ref}\ (z/z_{hub})^{0.11} = 1.4 * 30 * (16/16)^{0.11} = 42$ m/s

Where V_{ref} is the reference velocity taken from wind turbine class table from the average wind velocity of selected site. And, the value of z is equal to z_{hub} as the relevant gust velocity is at hub height.

3.5 FEA pre-processing

With the full definition of geometry and material properties, blade building process was began for FEA model. Due to the familiarity with the software the blade was designed using SolidWorks CAD package though it is possible for the modelling and analysis with Ansys. Because it is easy to import the geometry from SolidWorks to Ansys workbench, it is one of the most efficient ways for blade creation. The most desirable aerofoil was selected and the profile was imported into SolidWorks for geometry creation. The blade shape was created using eight aerofoil cross section profiles, as shown in Figure 14, with circular cross-section at the root where the blade leaves the hub. Firstly, aerofoil of blade was imported from XFOIL to SolidWorks which was scaled down and pasted on the plane at the span wise distance of 0.4 m from the base to the tip to have required chord length.

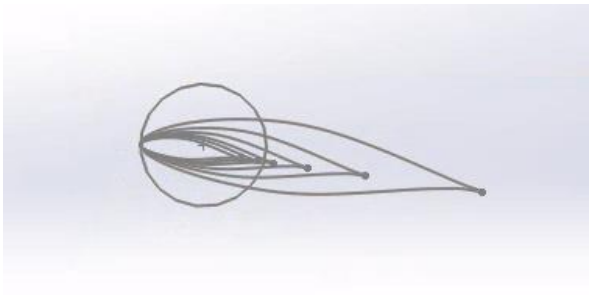

Figure 14: Aerofoil cross section profiles from SolidWorks

The blade was designed in SolidWorks as a lofted body for maximum flexibility and high computational efficiency within Ansys. Through the use of the lofted boss command, which produced parabolic tangencies in between profiles to produce a continuous, smooth surface, the curves were joined into a single body as shown in figure 15. The point on the leading edges and trailing edges were selected as a loft guiding point. Because the hub connection was beyond the scope of this study, the root part of the turbine, which is inside the hub, was excluded for the analysis.

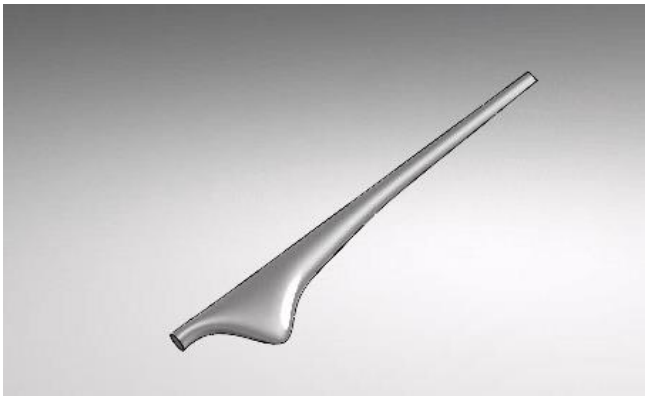

Figure 15: Lofted turbine blade model from SolidWorks

The fundamental model was laid out by using ANSYS software to create a comprehensive and precise composite blade. Firstly, the engineering data was set with the generation of new material as there is no pre-set properties of flax/pp composite in ANSYS. The density, orthographic elasticity, stress limit and strain limit were set. As the mixture was composite material the yield strength and ultimate strength was calculated and provided and S-N curve was defined as shown in figure 16.

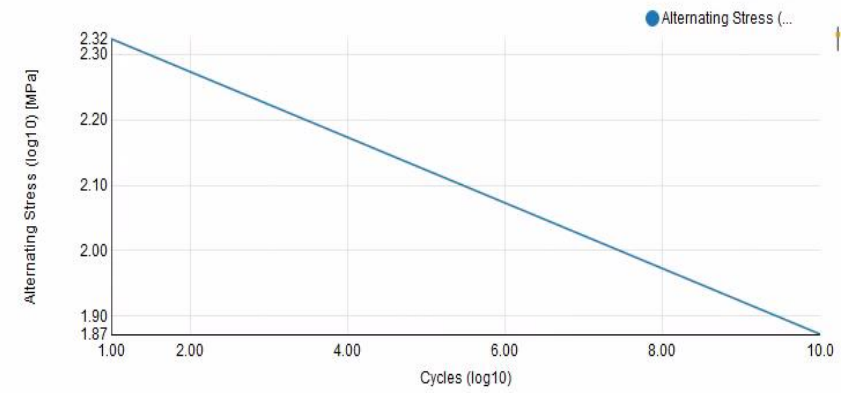

Figure 16: Log-log S-N curve

After the assignment of material properties, geometry was imported from the SolidWorks as IGES file. In the model section, the thickness of shell material was assigned as 3.2 mm and the geometry was meshed using 8-node SHELL 281 element. The SHELL 281 element in ANSYS makes up the majority of this three-dimensional finite element model. This kind of element is used to examine shell structures that are thin to fairly thick. It is suitable for both linear and non-linear cases since non-linear test takes variation in shell thickness into consideration (Gupta, 2013).

The default mesh generated contained 1097 nodes and 1983 elements and had the average quality of mesh as 63.78%. Then, all of the faces were assigned with a quadrilateral face mesh

by switching the element order to quadratic while the multi-zone quadrilateral mesh was applied on the leading and trailing edge to improve mesh quality. Because the triangle element models the reaction as extremely stiff, it was not employed during meshing. Also, quadrilateral element captures the structural response more accurately than tetrahedral one and was applied. Mesh was then refined to have the mesh which provides more accurate result by changing the element size and looking into the quality of mesh as output. Table 8 below shows the total number of nodes and elements present and the quality of mesh with different element size.

Table 8: Details of Mesh

Mesh	**Element size (mm)**	**Nodes**	**Elements**	**Mesh quality (%)**
Default	111.46	1097	1983	63.78
1	50	2066	682	96.64
2	20	11,510	3824	98.96
3	10	43,985	14,657	87.56

Due to higher simulation time meshing was not done for the element with size less than 10 mm. Among the meshing with four different element size the mesh quality was higher for the mesh with the element size of 20 mm. So, 8 node shell 281 element of size 20 mm was taken.

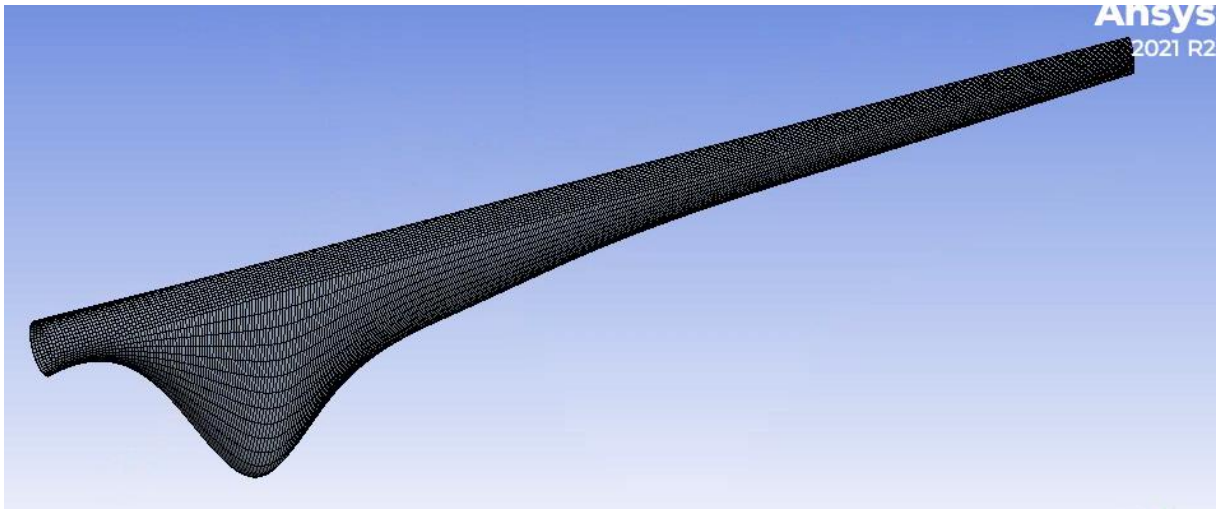

Figure 17: Mesh of blade model

Following material setup and mesh input, boundary condition was setup in model with four types of load as:

1. Fixed support at the blade root edge as it is fixed to the hub

2. Lift force perpendicular to blade
3. Drag force parallel to blade
4. Gravitational load
5. Centrifugal load

The mass of the blade and its surface area was taken from the SolidWorks as 61.62 kg and 1.69m^2.

$$Lift\ force\ =\ L = \frac{1}{2} C_L \rho A V^2 = \frac{1}{2} * 1.254 * 1.225 * 1.69 * 42^2\ =\ 2290\ N$$

$$Drag\ force = D = \frac{1}{2} C_D \rho A V^2\ =\ \frac{1}{2} * 0.013 * 1.225 * 1.69 * 42^2 =\ 23.7\ N$$

$$F_g =\ m_{blade}.g = 61.6\ * 9.81 =\ 604\ \text{N}$$

$$F_c =\ m_{blade}\omega^2 x = 61.6 * 26.18^2 * 1.07 = 45\ kN$$

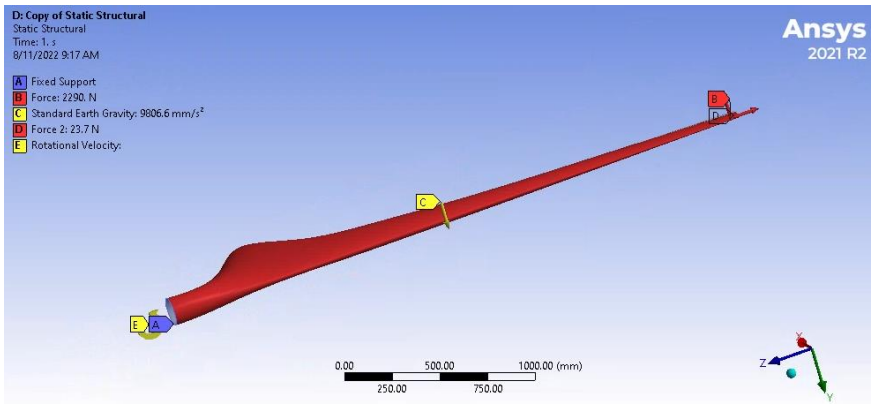

Figure 18: Load on blade at horizontal position

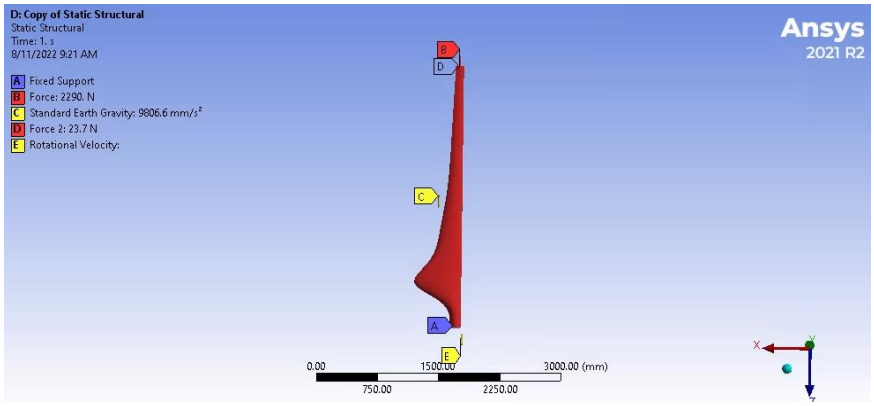

Figure 19: Load on blade at topmost position

With the definition of boundary condition the model was solved and deflection, equivalent stress, factor of safety for structural and fatigue failure, fatigue life and the damage accumulated. For fatigue analysis, stress life method was used with fully reverse loading (tension-compression).

4.0 Results and discussion

4.1 Result of structural analysis of blade

As the blade of turbine rotates gravitational force act perpendicular to the rotor blade when the blade is parallel to the ground. But when the blade is at the vertical topmost position this load will cause compression in the blade while it is at the bottommost position it leads to the tensile force in blade. So, structural and fatigue analysis was performed at three different load condition.

Case 1: Blade at horizontal position with shell thickness 3.2 mm

Figures show the equivalent alternating stress distribution and the deflection on pressure side of turbine blade. The maximum value of alternating stress was 201.42 MPa which occurred at the root of blade where it is fixed to the hub. The deflection of the turbine blade at the tip region was found as 440.81 mm which is quite high as it is free to move under the application of loads.

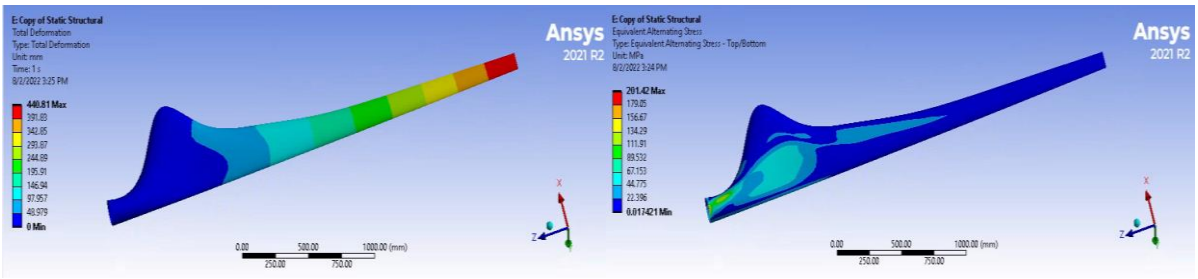

Figure 20: Deformation and equivalent stress on blade at horizontal position with shell thickness 3.2 mm

Case 2: Blade at topmost position with shell thickness 3.2 mm

When the blade was at top position the total deformation acting on the blade found to be 497.25 mm which is higher than when it was at horizontal position and the maximum equivalent alternating stress was 184.22 MPa. Although the pattern of stress distribution and deformation is similar to the first load condition.

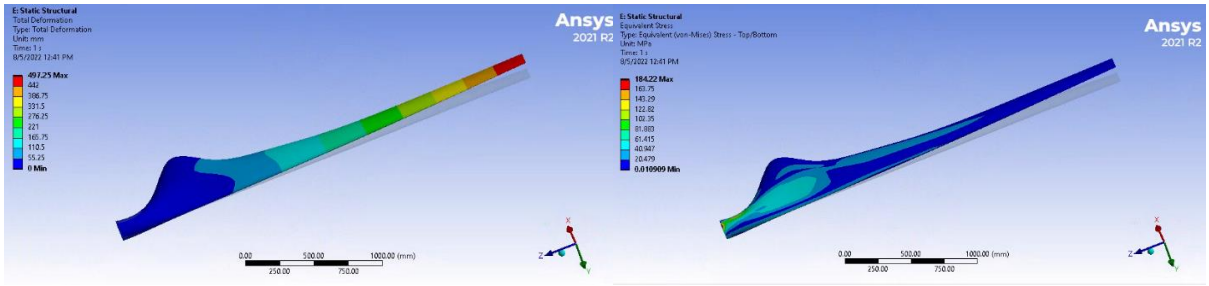

Figure 21: Deformation and equivalent stress on blade at topmost position with shell thickness 3.2 mm

Case 3: Blade at bottommost position with shell thickness 3.2 mm

In bottommost position there was not much change in the value for deformation and Von-mises stress as compare to its upmost position which was 497.96mm and 184 MPa.

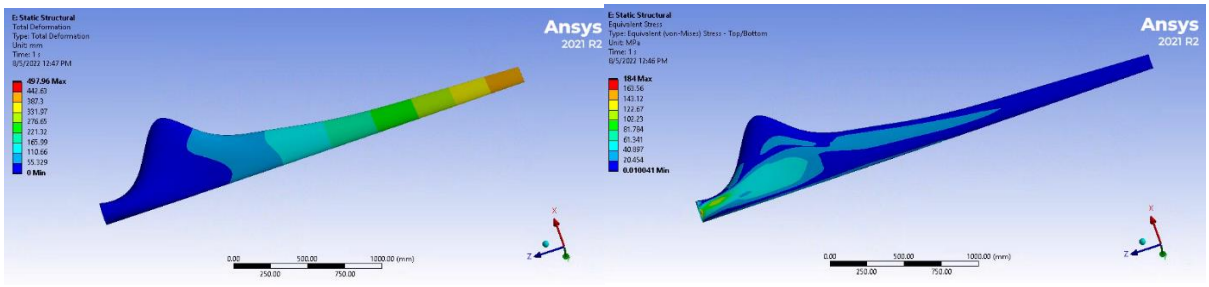

Figure 22: Deformation and equivalent stress on blade at bottommost position with shell thickness 3.2 mm

The stress concentration was larger on the surface with a wide cross section area, where the danger factor during operation is relatively significant. The deformation was greatest towards the tip of the rotor blade because it serves as a cantilever beam. Although the blade pre-bending structure mitigated much of the distortion, the blade might still collide with the wind turbine tower. The equivalent von Mises stress determined from static analysis served as the foundation for blade fatigue study.

4.2 Result of fatigue analysis of blade

The load signal was used to conduct the fatigue analysis, which comprises calculating fatigue life, damage, and factor of safety, after the statistical analysis. In this instance, the Von-mises stresses served as stress components together with the Goodman criteria for mean stress adjustment and the stress life approach.

Fatigue life

If the loading is constant amplitude, fatigue life is the number of cycles till the part fails due to fatigue. If the load is not constant, this is the number of load steps before failure.

Fatigue damage

The correlation between the estimated number of cycles to fail and the reference number of cycles over its design lifespan is represented by fatigue degradation or damage (Vidya and Christina, 2020) according to Miner's rule. The fatigue damage value greater than one means the blade will not survive till its design life.

Fatigue safety factor

This terminology is used to assess fatigue strength and anticipate if a component will break over its design life span due to cyclic stress in an event. The maximum value for this in ANSYS is 15. Factor of safety less than one indicates the blade failure before reaching design life (Zarrin-Ghalami and Fatemi, 2012).

Case 1: Blade at horizontal position with shell thickness 3.2 mm

At first, the blade with the shell thickness of 3.2mm, fatigue analysis was performed. The design life of the turbine blade ranges from 10^8-10^9 cycles so the design life of 10^9 was taken. Result showed that after 424.77 cycles the blade will start to fail on the suction side from the point where it is connected to hub. From the analysis it can be seen that the blade cannot withstand the load at extreme wind condition and damage will occur after certain cycle. Maximum damage will occur on circular portion at blade root where it is connected to the hub on the suction side with the value of $2.34*10^6$ which is extremely high while in most of the parts damage is very less with the value of 0.1.

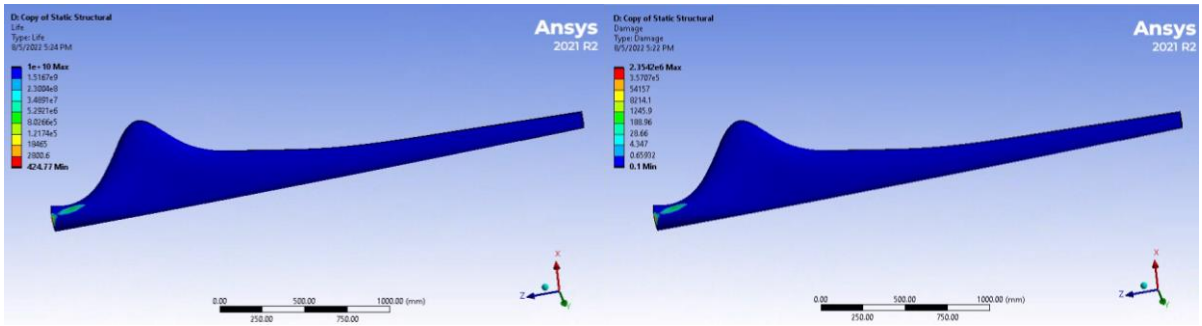

Figure 23: Fatigue life and damage on blade at horizontal position with shell thickness 3.2 mm

Factor of safety was analysed to have look on how safe the blade was from fatigue failure. According to IEC 1400-1, for the blade to be safe from fatigue failure with an extreme gust event, the factor of safety of 1.15 is needed to prevent the consequences from failure.In

ANSYS, value less than one represents the failure. And, the result shows that minimum value of factor of safety is 0.48 which is quite below the range for it to be fail safe.

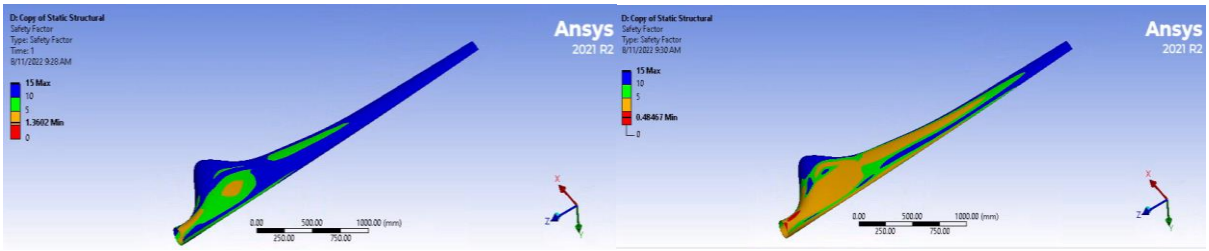

Figure 24: Structural and fatigue safety factor for blade at horizontal position with shell thickness 3.2 mm

Case 1: Blade at horizontal position with shell thickness 5 mm

So the blade was analysed again by changing the shell thickness to 5 mm. With an small increase in the thickness of the blade the deformation of the blade reduced by large amount although the pattern of the deformation was similar. For the load case I, the maximum total value of deformation found to be 298.88 mm while the equivalent alternating stress reduced from 201.42 to 111.12 MPa.

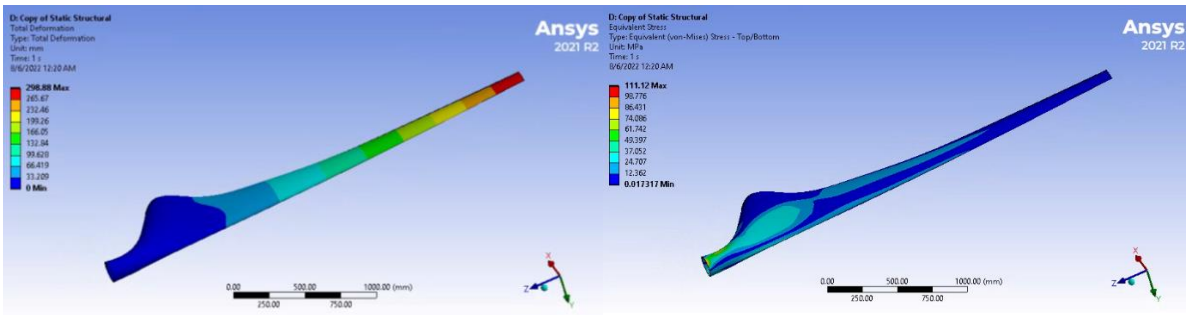

Figure 25: Deformation and equivalent stress on blade at horizontal position with shell thickness 5 mm

Safety factor for ultimate load ranges from 1.35 to 1.45 is required. For the 5 mm thickness blade the minimal value of safety factor for structural failure was 2.11 while for the fatigue analysis, the safety factor of 0.75 at the circular aerofoil connected to the hub while towards the tip it is more than one. So, it is statically safe. But, the value for the lower fatigue safety factor is still below the value required for it to be safe.

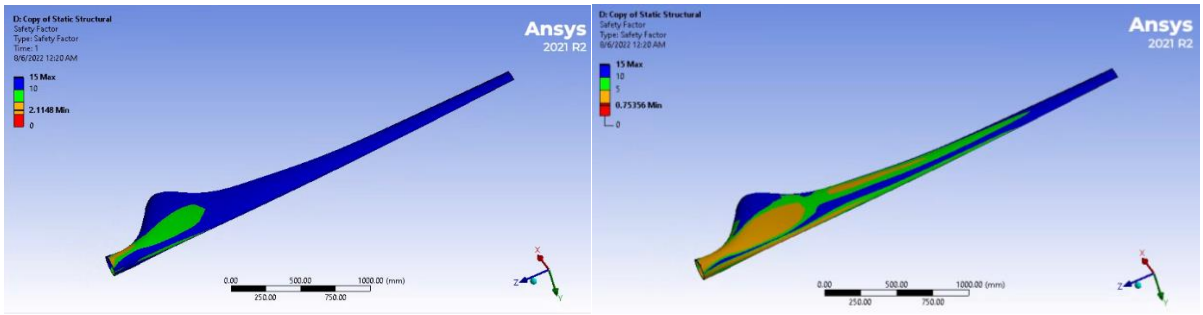

Figure 26: Structural and fatigue safety factor on blade at horizontal position with shell thickness 5 mm

The choosen blade had minimal damage of 0.1 and it will survive its design life apart from the section on the suction side at the root with life of $3.48*10^6$ and damage as 286.79. The damage is still greater than one which means that the blade will fail before it's design life.

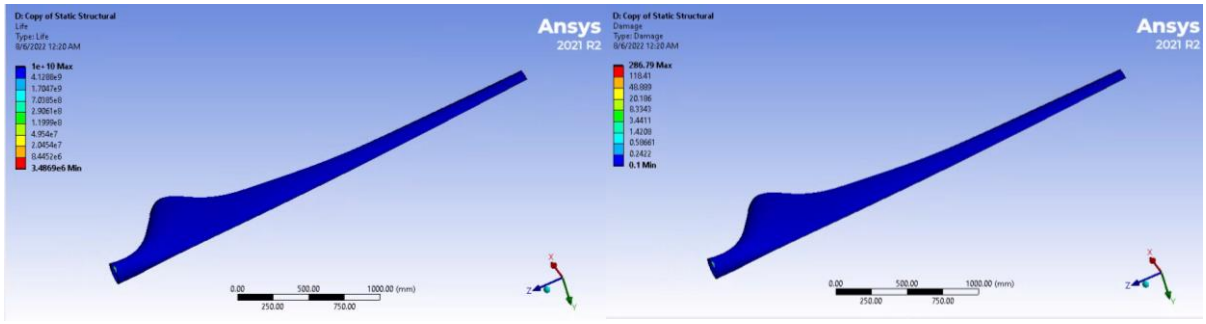

Figure 27: Fatigue life and damage on blade at horizontal position with shell thickness 5 mm

Further analysis was done by changing the thickness to have optimal thickness at which its safety factor will be greater than one. With the sheet thickness of 7mm the result for blade life, damage and factor of safety were shown in the figure.

Case 1: Blade at horizontal position with shell thickness 7 mm

In the horizontal position, the deformation, equivalent stress, safety factors, life and damage in blade was resolved. The deflection and von-mises stress of blade was found as 211.28 mm and 75.338 MPa. The minimum value of ultimate load safety factor was 3.1993 and for fatigue it was 1.11. Both of these value is greater than the mimimal safety factor required. So it is safe from fatigue failure. With that value of alternating stress, it has life of $8.27 *10^9$ and maximum damage of 0.12 which is below one.

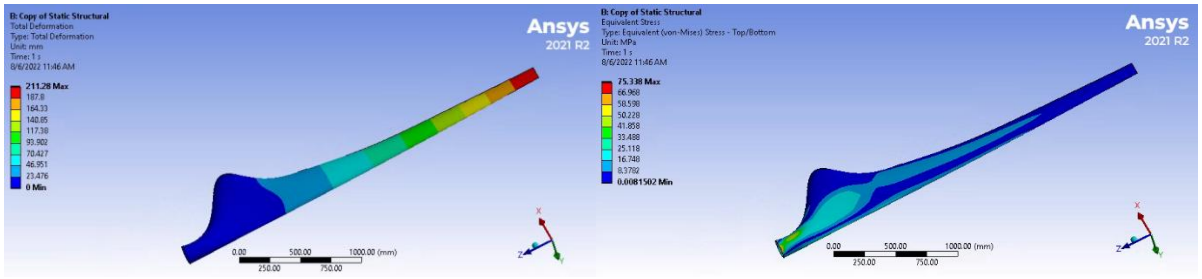

Figure 28: Deformation and equivalent stress on blade at horizontal position with shell thickness 7 mm

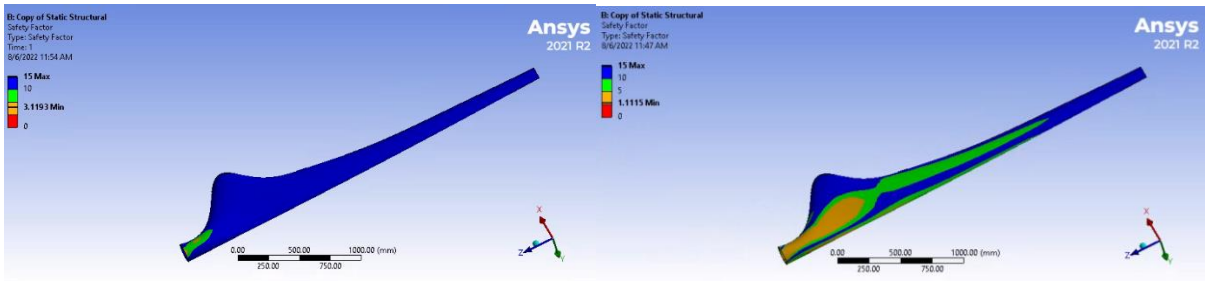

Figure 29: Structural and fatigue safety factor on blade at horizontal position with shell thickness 7 mm

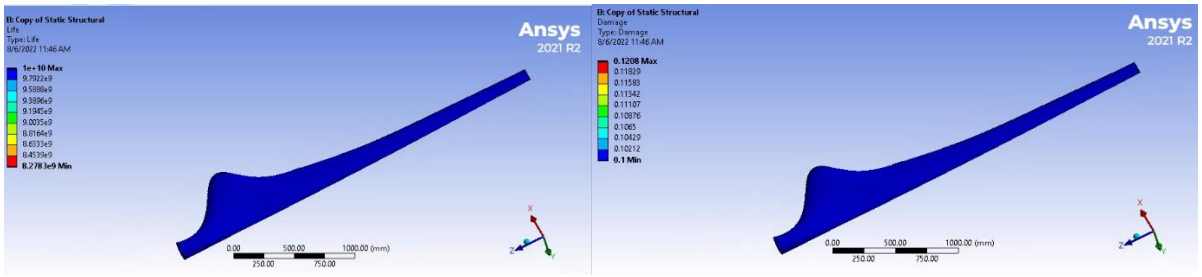

Figure 30: Fatigue life and damage on blade at horizontal position with shell thickness 7 mm

Case 2: Blade at topmost position with shell thickness 7 mm

With the different load condition at the topmost position as gravitational load acts along the blade span, ultimate load and fatigue analysis was done. With the deflection and von-mises stress value as 217.25 and 79.188 MPa, mimimum value of ultimate load safety factor was 2.96 and for fatigue it was 1.06. Even though these safety factors were less than the one with blade parallel to surface but it is still greater than the mimimal safety factor required. So it is safe from both structural and fatigue failure. With that value of alternating stress, it has life of $3.05*10^9$ and maximum damage of 0.32 which is below one.

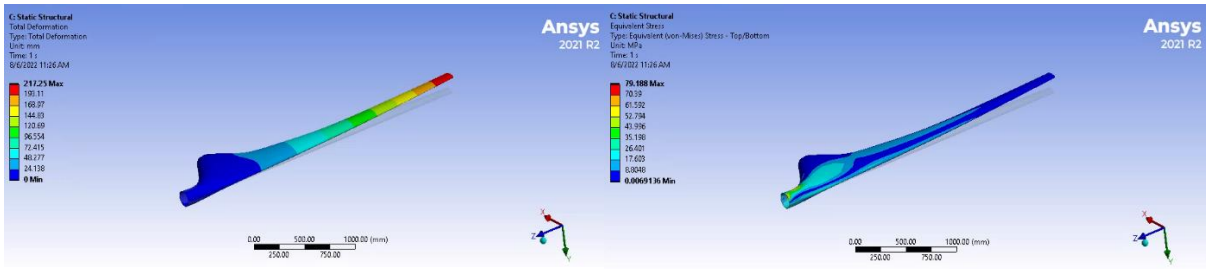

Figure 31: Deformation and equivalent stress on blade at topmost position with shell thickness 7 mm

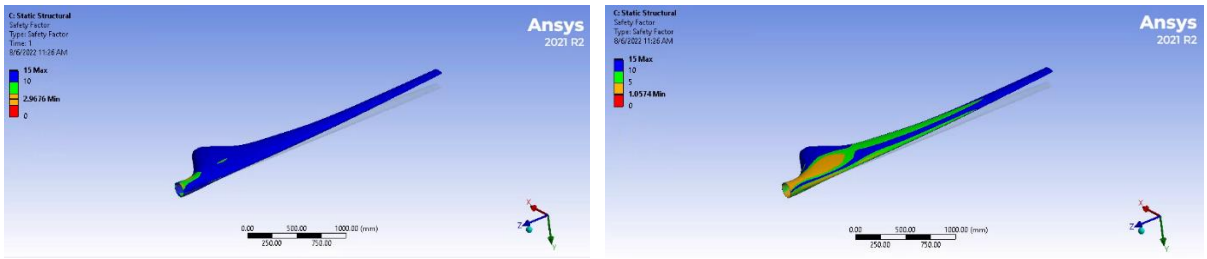

Figure 32: Structural and fatigue safety factor on blade at topmost position with shell thickness 7 mm

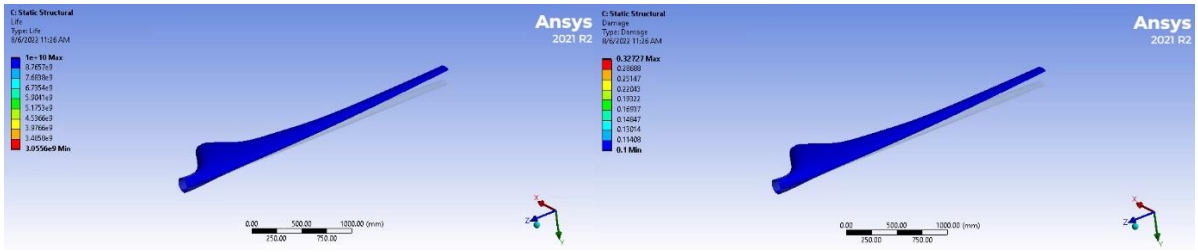

Figure 33: Fatigue life and damage on blade at topmost position with shell thickness 7 mm

5.0 Conclusion

This thesis presented the design and analysis of small horizontal axis wind turbine of 5kW power generation capacity. The aerodynamic characteristics of four types of aerofoil: NACA 63(4)-421, NACA 2421, LS (1)-0417, LS (1)-0421 has been analysed using XFOIL software to evaluate its performance. The most effective aerofoil was NACA 63(4)-421 since the L/D ratio is higher for this profile at the most effective attack angle of 8.5 degree. The blade design parameter was evaluated and aerofoil profile was generated by exporting the coordinate values from XFOIL to SOLIDWORKS and scaled and lofted to create the blade model for describing the actual shape for further analysis. A composite blade with flax as fibre and polypropylene as matrix was taken due to its recyclable properties and high fatigue strength than other natural fibre composites. As the properties of composites will be different than that of the single material and it depends on the percentage of fibre in composite, 40% flax fibre fraction was taken. The material properties like elasticity, stress and strain values for orthographic fibre-matrix composite was determined. The blade was analysed against the extreme gust loading

condition. With the determination of the applicable load on blade, static and fatigue analysis was conducted in Finite Element analysis software ANSYS. The result from the analysis shows that the alternating stress will be maximum towards the section with higher cross-sectional area near to the root and in the area where it is connected to the hub. With the shell thickness of 3.2 mm total deformation, stress distribution and structural safety factor was determined. Structurally the blade was in safe limit. So, the fatigue analysis was performed as the next step to check whether the blade will handle the fatigue stress or not. Result shows that the blade will start to fracture immediately from the root on the suction side and damage will be extremely high with fatigue factor of safety well below one. It was concluded that even though the structure is structurally safe it might not necessarily be safe from fatigue failure. With the shell thickness of 5 mm, the fatigue failure starts after certain life below the blade design life. And, with shell thickness of 7 mm it will survive from the fatigue failure throughout its design life with very less damage. Since the total load acting on the blade will varied and so alternating stress as gravitational force will act at different direction in different position of blade. So, the analysis was performed again with the blade at the topmost position. The result showed that the blade will survive the fatigue failure at this position as well with the value of factor of safety greater than one. But with increasing the thickness of the weight of the blade increases and so does the cost. Since the structure and fatigue failure is mostly towards the root of the blade near to the hub it is concluded that the blade needs to be optimized with greater thickness towards the root and the profile of smaller thickness at the tip. Finally, to accurately assess fatigue failure while designing the rotor blades, simple and trustworthy dynamic models are needed.

6.0 Future work

This thesis presented the evaluation of blade aerodynamic performance derived from BEM theory along with static and fatigue analysis. Although the analysis was performed to determine the behaviour of blade, there will still some deviation in real life which make it essential to perform the full scale manufacturing and testing of blade experimentally in the laboratory to validate the accuracy of developing designs and computer models. Due to the complexity of the design and requirement of greater simulation time during analysis, only a single blade with simple shell structure was used for the analysis. Additionally, a small mesh is necessary for the full wind turbine blades simulation. As there is restriction in memory in personal computer it requires high configuration computers to run the simulation. Also, time limitation and difficulty in data acquiring restricted the dynamic fatigue analysis of the turbine

blades with different load cases. Among the eight load cases defined by IS-61400-2 only parked condition of the blade was taken during analysis. In the future, it is suggested to evaluate the blade with rest of load cases to make sure that blade will be safe when subjected to the rotational dynamic load along with unsteady wind velocity. Here, the analysis was performed with the material properties of composite ply with 45°/-45° orientation. Since mechanical properties value differs with different orientation of fibres in composite, in the future, blade can be analysed with different orientation and stack up in the structure. As the blades were subjected to varying load it is recommended to use different computer software like FAST, MATLAB to determine whether the blade is within safe limit or not for both structural and fatigue damage.

7.0 Reference

[1] Adaramola, M. ed., (2021). *WIND TURBINE TECHNOLOGY: principles and design.* S.L.: Apple Academic Press.

[2] Adeseye Adeyeye, K., Ijumba, N. and Colton, J. (2021). The Effect of Number of Blades on the Efficiency of a Wind Turbine. In: *2021 11th International Conference on Future Environment and Energy*. Tokyo, Japan: IOP Publishing Ltd.

[3] Advantages/Disadvantages of two-bladed windmill 2016 Available online: https://engineering.stackexchange.com/questions/10754/advantages-disadvantages-of-two-bladed-windmill. [Accessed: 30-Oct-2019].

[4] Andersons, J., Spārniņš, E. and Joffe, R. (2009). Uniformity of filament strength within a flax fiber batch. *Journal of Materials Science*, 44(2), pp.685–687. doi:10.1007/s10853-008-3171-3.

[5] Aykan, M. (2005). *Vibrational fatigue analysis of equipments used in A erospace*. Undergraduate dissertation. pp.15–28.

[6] Benham, A., Thyagarajan, K., John, S.J. and Prakash, S. (2013). Structural Analysis of a Wind Turbine Blade. *Advanced Materials Research*, 768, pp.40–46. doi:10.4028/www.scientific.net/amr.768.40.

[7] Bensadoun, F., Vallons, K.A.M., Lessard, L.B., Verpoest, I. and Van Vuure, A.W. (2016). Fatigue behaviour assessment of flax–epoxy composites. *Composites Part A: Applied Science and Manufacturing*, 82, pp.253–266. doi:10.1016/j.compositesa.2015.11.003.

[8] Bharambe, V.R. and Bharambe, C.R. (2018). Reactive Power Improvement Using STATCOM in Grid Connected Wind Energy System. *International Journal for Scientific*

Research and Development, 6, pp.300–302.

[9] Brøndsted, P., Lilholt, H. and Lystrup, A. (2005). COMPOSITE MATERIALS FOR WIND POWER TURBINE BLADES. *Annual Review of Materials Research*, [online] 35(1), pp.505–538. doi:10.1146/annurev.matsci.35.100303.110641.

[10] Budynas, R.G., J Keith Nisbett and Joseph Edward Shigley (2020). *Shigley's mechanical engineering design*. New York, Ny: Mcgraw-Hill Education.

[11] Burton, T. (2011). *Wind energy handbook*. Chichester, West Sussex: Wiley.

[12] Cao, H. (2011). *Aerodynamic Analysis of Small Horizontal Axis Wind Turbines by using 2D and 3D CFD modelling*. MSc (by Research). pp.1–5.

[13] Christensen, R.M. (2005). *Mechanics of composite materials*. Mineola, N.Y.: Dover Publications.

[14] Clausen, P.D. and Wood, D.H. (1999). Research and development issues for small wind turbines. *Renewable Energy*, 16(1-4), pp.922–927. doi:10.1016/s0960-1481(98)00316-4.

[15] Corbière-Nicollier, T., Gfeller Laban, B., Lundquist, L., Leterrier, Y., Månson, J.-A. .E and Jolliet, O. (2001). Life cycle assessment of biofibres replacing glass fibres as reinforcement in plastics. *Resources, Conservation and Recycling*, 33(4), pp.267–287. doi:10.1016/s0921-3449(01)00089-1.

[16] DESIGN AND ANALYSIS OF HORIZONTAL AXIS WIND TURBINE BLADE. (2016). *International Journal of Modern Trends in Engineering & Research*, 3(9), pp.126–132. doi:10.21884/ijmter.2016.3053.skkij.

[17] Dominy, R., Lunt, P., Bickerdyke, A. and Dominy, J. (2007). Self-starting capability of a Darrieus turbine. *Proceedings of the Institution of Mechanical Engineers, Part A: Journal of Power and Energy*, 221(1), pp.111–120. doi:10.1243/09576509jpe340.

[18] Dong, C. (2017). Review of natural fibre-reinforced hybrid composites. *Journal of Reinforced Plastics and Composites*, 37(5), pp.331–348. doi:10.1177/0731684417745368.

[19] Eduard Muljadi, H Edward Mckenna and National Renewable Energy Laboratory (U.S (2001). *Power quality issues in a hybrid power system : preprint*. Golden, Co: National Renewable Energy Laboratory, September.

[20] E Hau (2013). *Wind turbines : fundamentals, technologies, application, economics*. Heidelberg ; New York: Springer.

[21] Evans, S., Dana, S., Clausen, P. and Wood, D. (2020). A simple method for modelling fatigue spectra of small wind turbine blades. *Wind Energy*. doi:10.1002/we.2588.

[22] Gasch, R. and Jochen Twele (2012). *Wind power plants fundamentals, design, construction and operation*. Berlin Heidelberg Springer.

[23] Guideline for the Certification of Wind Turbines, Germanischer Lloyd (GL) Std., 2010.

[24] Gupta, N. (2013). *Structural Study and Parametric Analysis on Fatigue Damage of a Composite Rotor Blade3*. MSc Thesis.

[25] Gurit, "Guide to Composites". www.gurit.com

[26] Habali, S.M. and Saleh, I.A. (2000). Local design, testing and manufacturing of small mixed airfoil wind turbine blades of glass fiber reinforced plastics. *Energy Conversion and Management*, 41(3), pp.249–280. doi:10.1016/s0196-8904(99)00103-x.

[27] Herrera-Franco, P.J. and Valadez-González, A. (2004). Mechanical properties of continuous natural fibre-reinforced polymer composites. *Composites Part A: Applied Science and Manufacturing*, 35(3), pp.339–345. doi:10.1016/j.compositesa.2003.09.012.

[28] Huque, Z., Zemmouri, G., Harby, D. and Kommalapati, R. (2012). Optimization of Wind Turbine Airfoil Using Nondominated Sorting Genetic Algorithm and Pareto Optimal Front. *International Journal of Chemical Engineering*, 2012, pp.1–9. doi:10.1155/2012/193021.

[29] Hyams M.A (2012). *Wind energy in the built environment*. Elsevier Ltd.

[30] IEA. (2021). *World Energy Outlook – Topics*. [online] Available at: http://www.iea.org/weo.

[31] International Electrotechnical Commission and International Electrotechnical Commission. Technical Committee 88 (2014). *Wind turbines. Part 1, Design requirements*. Geneva: International Electrotechnical Commission.

[32] IRENA (2019), Future of wind: Deployment, investment, technology, grid integration and socio-economic aspects (A Global Energy Transformation paper), International Renewable Energy Agency, Abu Dhabi.

[33] Irvine, T. (2018). *RAINFLOW CYCLE COUNTING IN FATIGUE ANALYSIS Revision B*. [online] Available at: http://www.vibrationdata.com/tutorials2/rainflow_counting_revB.pdf [Accessed 1 Aug. 2022].

[34] Jenkins J, Rhoads-Weaver H, Forsyth T, Summerville B, Baranowski R, Rife B. SMART Wind Roadmap, Distributed Wind Energy Association (DWEA). (United States): Durango, CO; 2016.

[35] Karthikeyan, N. and Suthakar, T. (2016). Computational studies on small wind

turbine performance characteristics. *Journal of Physics: Conference Series*, 759, p.012087. doi:10.1088/1742-6596/759/1/012087.

[36] Kellersztein, I. and Dotan, A. (2015). Chemical surface modification of wheat straw fibers for polypropylene reinforcement. *Polymer Composites*, 37(7), pp.2133–2141. doi:10.1002/pc.23392.

[37] Kerrigan S 2018 The Scientific Reason Why Wind Turbines Have 3 Blades Available online: https://interestingengineering.com/the-scientific-reason-why-wind-turbines-have-3-blades. [Accessed: 30-Oct2018].

[38] Kishore, R.A., Coudron, T. and Priya, S. (2013). Small-scale wind energy portable turbine (SWEPT). *Journal of Wind Engineering and Industrial Aerodynamics*, 116, pp.21–31. doi:10.1016/j.jweia.2013.01.010.

[39] Kong, C., Bang, J. and Sugiyama, Y. (2005). Structural investigation of composite wind turbine blade considering various load cases and fatigue life. *Energy*, [online] 30(11-12), pp.2101–2114. doi:10.1016/j.energy.2004.08.016.

[40] Kong, C., Kim, M. and Park, G. (2014). A study on aerodynamic and structural design of high efficiency composite blade of 1 MW class HAWTS considering fatigue life. *Advanced Composite Materials*, 24(1), pp.67–83. doi:10.1080/09243046.2014.881630.

[41] Kumar, M.S., Krishnan, A.S. and Vijayanandh, R. (2018). Vibrational Fatigue Analysis of NACA 63215 Small Horizontal Axis Wind Turbine blade. *Materials Today: Proceedings*, 5(2), pp.6665–6674. doi:10.1016/j.matpr.2017.11.323.

[42] Le Duigou, A. and Baley, C. (2014). Coupled micromechanical analysis and life cycle assessment as an integrated tool for natural fibre composites development. *Journal of Cleaner Production*, 83, pp.61–69. doi:10.1016/j.jclepro.2014.07.027.

[43] Li-Hua, Z., Ming, L. and Tie, L. (2013). Study on the Aerodynamic Performance of Blade Airfoil of Vertical Axis Wind Turbine at Low Reynolds Number. *Information Technology Journal*, 12(14), pp.3042–3045. doi:10.3923/itj.2013.3042.3045.

[44] Maalawi, K.Y. and Badr, M.A. (2003). A practical approach for selecting optimum wind rotors. *Renewable Energy*, 28(5), pp.803–822. doi:10.1016/s0960-1481(02)00028-9.

[45] Marcal, P.V. and Yamagata, N. (2016). *Design and Analysis of Reinforced Fiber Composites*. Cham Springer International Publishing.

[46] Mathew, S. (2011). *Advances in wind energy and conversion technology*. Berlin: Berlin Heidelberg Springer, pp.159–161.

[47] Megraw S 2012 Why don't wind turbines have more than 3 blades? Available online: aspxexplorecuriocite.org/Explorer/ArticleId/193/why-dont-wind-turbines-have-more-

than-3-blades-193. [Accessed: 30-Oct-2019].

[48] Mishnaevsky, L., Branner, K., Petersen, H., Beauson, J., McGugan, M. and Sørensen, B. (2017). Materials for Wind Turbine Blades: An Overview. *Materials*, [online] 10(11), p.1285. doi:10.3390/ma10111285.

[49] Mohd Bakhori, S.N., Zaki Hassan, M., Abdul Aziz, S., Md. Fadzulah, S. and Ahmad, F. (2018). Tensile properties of jute-polypropylene composites. *Chemical Engineering Transactions*, 63, pp.727–732. doi:10.3303/CET1863122.

[50] Muhsen, H., Al-Kouz, W. and Khan, W. (2019). Small Wind Turbine Blade Design and Optimization. *Symmetry*, 12(1), p.18. doi:10.3390/sym12010018.

[51] Nguyen, L. and Metzger, M. (2015). Enhanced energy capture by a vertical axis wind turbine during gusty winds in an urban/suburban environment. *Journal of Renewable and Sustainable Energy*, 7(5), p.053118. doi:10.1063/1.4934585.

[52] Notta-Cuvier, D., Lauro, F., Bennani, B. and Nciri, M. (2015). Impact of natural variability of flax fibres properties on mechanical behaviour of short-flax-fibre-reinforced polypropylene. *Journal of Materials Science*, 51(6), pp.2911–2925. doi:10.1007/s10853-015-9599-3.

[53] Rao, K.R. (2019). *Wind energy for power generation: meeting the challenge of practical implementation*. Cham, Switzerland: Springer.

[54] R. T. Griffiths, The effect of aerofoil characteristics on windmill performance, The Aeronautical Journal, 81 (July, 1977), pp. 322-6.

[55] Saheb, D., Koussa, M. and Hadji, S. (2014). Technical and Economic Study of a Stand-Alone Wind Energy System for Remote Rural Area Electrification in Algeria. *Renewable Energy and Power Quality Journal*, pp.638–643. doi:10.24084/repqj12.439.

[56] Sarkar, Md., Julai, S., Wen Tong, C. and Toha, S. (2019). Effectiveness of Nature-Inspired Algorithms using ANFIS for Blade Design Optimization and Wind Turbine Efficiency. *Symmetry*, 11(4), p.456. doi:10.3390/sym11040456.

[57] Singh, R.K. and Ahmed, M.R. (2013). Blade design and performance testing of a small wind turbine rotor for low wind speed applications. *Renewable Energy*, 50, pp.812–819. doi:10.1016/j.renene.2012.08.021.

[58] Song, D., Fan, X., Yang, J., Liu, A., Chen, S. and Joo, Y.H. (2018). Power extraction efficiency optimization of horizontal-axis wind turbines through optimizing control parameters of yaw control systems using an intelligent method. *Applied Energy*, 224, pp.267–279. doi:10.1016/j.apenergy.2018.04.114.

[59] Sutherland, H.J. (2000). A summary of the fatigue properties of wind turbine

materials. *Wind Energy*, 3(1), pp.1–34. doi:10.1002/1099-1824(200001/03)3:1<1::aid-we28>3.0.co;2-2.

[60] Tabesh, A. and Iravani, R. (2006). Small-Signal Dynamic Model and Analysis of a Fixed-Speed Wind Farm—A Frequency Response Approach. *IEEE Transactions on Power Delivery*, 21(2), pp.778–787. doi:10.1109/tpwrd.2005.858801.

[61] Tavner, P.J., Xiang, J. and Spinato, F. (2007). Reliability analysis for wind turbines. *Wind Energy*, [online] 10(1), pp.1–18. doi:10.1002/we.204.

[62] Tenghiri, L., Khalil, Y., Abdi, F. and Bentamy, A. (2018). Optimum design of a small wind turbine blade for maximum power production. *IOP Conference Series: Earth and Environmental Science*, 161, p.012008. doi:10.1088/1755-1315/161/1/012008.

[63] Tirkey A, Sarthi Y, Patel K, Sharma R, Sen P K, and Engg M 2014 Study on the effect of blade profile, number of blade, Reynolds number, aspect ratio on the performance of vertical axis wind turbine Int. J. Sci. Eng. Technol. Res., vol. 3, no. 12, pp. 3183–3187.

[64] Tong, W. ed., (2011). Wind power generation and wind turbine design. *Choice Reviews Online*, 48(07), pp.48–390448–3904. doi:10.5860/choice.48-3904.

[65] UCL (2022). *Opinion: Renewables are cheaper than ever – so why are household energy bills only going up?* [online] UCL News. Available at: https://www.ucl.ac.uk/news/2022/jan/opinion-renewables-are-cheaper-ever-so-why-are-household-energy-bills-only-going.

[66] Van den Oever, M.J.A., Bos, H.L. & van Kemenade, M.J.J.M. Influence of the Physical Structure of Flax Fibres on the Mechanical Properties of Flax Fibre Reinforced Polypropylene Composites. *Applied Composite Materials* 7, 387–402 (2000). https://doi.org/10.1023/A:1026594324947

[67] Verpoest, A general introduction to composites, highlighting the advantages of flax and hemp composites, In : Reux and Verpoest, vol.2012, pp.15-37

[68] Vidya, M.S. and Christina, K.V.M. (2020). Fatigue Life, Fatigue Damage, Fatigue Factor of Safety, Fatigue Sensitivity, Biaxiality Indication and Equivalent Stress of a Radial Connecting Rod. *International Research Journal of Engineering and Technology (IRJET)*, 07(09).

[69] Wang S and Chen S 2008 Blade number effect for a ducted wind turbine J. Mech. Sci. Technol., vol. 22, pp. 1984–1992. [13] Rehman S, A.

[70] Xudong, W., Shen, W.Z., Zhu, W.J., Sørensen, J.N. and Jin, C. (2009). Shape optimization of wind turbine blades. *Wind Energy*, 12(8), pp.781–803.

doi:10.1002/we.335.

[71] Xu, Z.Q. (2014). Research on Material Thickness and Material Properties with Application of Sensors. *Advanced Materials Research*, 1021, pp.33–36. doi:10.4028/www.scientific.net/amr.1021.33.

[72] Yvonne Biyana, N. (2015). *Studies on Flax/ Polypropylene- Reinforced Composites for Automotive Applications*. Masters of Science (M. Sc.) in Textile Science. pp.44–46.

[73] ZARRIN-GHALAMI, T. and FATEMI, A. (2012). Cumulative fatigue damage and life prediction of elastomeric components. *Fatigue & Fracture of Engineering Materials & Structures*, 36(3), pp.270–279. doi:10.1111/j.1460-2695.2012.01720.x.